JOURNAL OF GEOPHYSICAL RESEARCH, VOL. 93, NO. D2, PAGES 1509–1527, FEBRUARY 20, 1988

Biomass-Burning Emissions and Associated Haze Layers Over Amazonia

M. O. ANDREAE,[1,2] E. V. BROWELL,[3] M. GARSTANG,[4] G. L. GREGORY,[3] R. C. HARRISS,[3] G. F. HILL,[3] D. J. JACOB,[5] M. C. PEREIRA,[6] G. W. SACHSE,[3] A. W. SETZER,[6] P. L. SILVA DIAS,[7] R. W. TALBOT,[3] A. L. TORRES,[8] AND S. C. WOFSY[5]

Biomass-burning plumes and haze layers were observed during the ABLE 2A flights in July/August 1985 over the central Amazon Basin. The haze layers occurred at altitudes between 1000 and 4000 m and were usually only some 100 to 300-m thick but extended horizontally over several 100 km. They could be traced by satellite imaging and trajectory studies to biomass burning at the southern perimeter of the Amazon Basin, with transport times estimated to be 1–2 days. These layers strongly influenced the chemical and optical characteristics of the atmosphere over the eastern Amazon Basin. The concentrations of CO, CO_2, O_3, and NO were significantly elevated in the plumes and haze layers relative to the regional background. The NO/CO ratio in fresh plumes was much higher than in the aged haze layers, suggesting that more than 80% of the NO_x in the haze layers had been converted to nitrate and organic nitrogen species subsequent to emission. The haze aerosol was composed predominantly of organic material, NH_4^+, K^+, NO_3^-, $SO_4^=$, and anionic organic species (formate, acetate, and oxalate). While the concentrations of most aerosol ions were substantially higher in the haze layers than in the regional background aerosol, the ratios between the aerosol ions in the haze layer aerosols were very similar to those in the boundary layer aerosol over the central Amazon region. Simultaneous measurements of trace gas and aerosol species in the haze layers made it possible to derive emission ratios for CO, NO_x, NH_3, sulfur oxides, and aerosol constituents relative to CO_2. Regional and global emission estimates based on these ratios indicate that biomass burning is an important contributor in the global and regional cycles of carbon, sulfur, and nitrogen species. Similar considerations suggest that photochemical ozone production in the biomass-burning plumes contributes significantly to the regional ozone budget.

INTRODUCTION

Biomass burning has been recognized as a significant source of CO_2 to the atmosphere: the input from this source has been estimated by *Seiler and Crutzen* [1980] to be about 2–4 Pg C yr^{-1} (Pg = petagram, 10^{15} g), comparable to the emissions from fossil fuel burning (about 5 Pg C yr^{-1}). Most biomass burning takes place in the tropical and subtropical regions, and much of the burning activity is limited to a "burning season," the timing of which is related to seasonal patterns and agricultural practices. In view of the temporal and spatial concentration of biomass-burning activity, it is not unexpected that its impact on the chemical and physical characteristics of the tropical atmosphere can be very pronounced, but because of the logistic difficulties of obtaining measurements in most of the affected regions, there are only a few studies which document this impact [*Crutzen et al.*, 1979, 1985; *Delmas*, 1982; *Greenberg et al.*, 1984; *Cachier et al.*, 1985]. However, evidence for the global impact of biomass burning has been found even over remote oceanic regions in studies of the abundance of soot carbon and other chemical tracers for biomass combustion [*Andreae*, 1983; *Andreae et al.*, 1984].

During the Amazon Boundary Layer Experiment (ABLE 2A), conducted during July/August 1985 in central Amazonia [*Harriss et al.*, this issue], we visually observed the presence of haze layers during many of the research flights. The frequency of occurrence and the density of these layers increased throughout the experiment, coinciding with an increase in biomass burning at the southern periphery of the Amazon Basin and with the frequency of air mass transport from the southeast [*Setzer and Pereira*, 1986]. We investigated the characteristics of these haze layers by remote and in situ measurements, using the broad range of instrumentation and sampling equipment installed in the NASA Electra research aircraft during ABLE 2A. In this paper we present the results of optical measurements by airborne lidar; of continuous in situ measurements of CO_2, CO, NO, and O_3; and of the analysis of discrete "grab" samples of atmospheric aerosols and acidic gases (HNO_3 and SO_2). From these measurements we derive estimates of the source fluxes of aerosol and gaseous materials from biomass burning in the tropics.

METHODS

Sampling and in situ measurements were conducted on the NASA Electra research aircraft, which was based in Manaus, Brazil, during the ABLE 2A experiment in July and August 1985. The sampling and analytical methods employed for the collection of data on the haze layers are described in detail in other publications by the members of the ABLE 2A science team: CO was determined by the DACOM laser absorption instrument [*Sachse et al.*, this issue]; CO_2 by a nondispersive infrared absorption instrument [*Wofsy et al.*, this issue]; NO by chemiluminescence

[1]Department of Oceanography, Florida State University, Tallahassee.
[2]Now at Max Planck Institute for Chemistry, Mainz, Federal Republic of Germany.
[3]NASA Langley Research Center, Hampton, Virginia.
[4]Department of Environmental Sciences, University of Virginia, Charlottesville.
[5]Center for Earth and Planetary Physics, Harvard University, Cambridge, Massachusetts.
[6]Department of Meteorology, Instituto de Pesquisas Espaciais, São José dos Campos, São Paulo, Brazil.
[7]Department of Meteorology, University of São Paulo, São Paulo, Brazil.
[8]NASA Wallops Flight Facility, Wallops Island, Virginia.

Paper number 7D0433.
0148-0227/88/007D-0433$05.00

[*Torres and Buchan*, this issue]; and ozone by NO chemiluminescence [*Gregory et al.*, this issue]. The airborne lidar system for measurements of ozone and aerosol distribution has been described by *Browell et al.* [this issue]. Aerosols and acidic gases were sampled with a filter-pack system, which collected large and fine particles separately on Nuclepore and Teflon filters, respectively [*Talbot et al.*, this issue]. The acidic gases were absorbed on the third stage, a K_2CO_3-impregnated paper filter. All analyses of these filters were made using ion chromatography [*Andreae et al.*, this issue]. Particulate organic carbon was determined by a combustion technique from quartz filters; black carbon was determined on the same filters using light absorption [*Andreae et al.*, 1984]. Total aerosol mass was measured with a quartz crystal microbalance impactor [*Talbot et al.*, this issue].

RESULTS AND DISCUSSION

Sampling Environment and Meteorological Conditions

The large-scale meteorological conditions prevailing during the experiment have been described by *Harriss et al.* [this issue] and the boundary layer meteorology by *Martin et al.* [this issue]. The data discussed here were collected during a series of flights in July and August 1985, most of which took place over large, almost completely undisturbed regions of Amazonian rain forest. Only near rivers and in the periphery of the few large inhabited areas (e.g., Manaus, Tabatinga, and Belém, see Figure 1) were signs of agricultural activity with associated burning observed. In order to obtain information on large-scale trends in the distribution of atmospheric constituents, we conducted survey flights which covered the region from the border between Brazil and Colombia (near 70°W) to the Atlantic coast (near 48°W) [*Harriss et al.*, this issue]. The experiment began in mid-July, after the onset of the dry season but during a period of relatively frequent precipitation. Air flow over the Amazon Basin south of the equator was predominantly from the east to southeast during this period as a result of the presence of the subtropical anticyclone, centered near 20°–25°S and 35°–45°W. On July 31 the remnants of a high-latitudinal upper level trough entered the southwestern part of the Amazon Basin, triggering instability and convective storms over the basin on August 2 and 3 [*Garstang et al.*, this issue]. During the course of the experiment, which ended on August 9, the overall frequency of precipitation decreased, with the exception of the disturbed episodes mentioned previously. The establishment of anticyclonic circulation over central Brazil introduced increasing amounts of air from the southeastern perimeter of the Amazon Basin into the study area. This was accompanied by increasing levels of atmospheric haze during the later part of the experiment. An example of the flow field near the end of the experiment is shown in the streamline map for August 9, 1985 (1200 UT) at 700 hPa (Figure 1). This level is near a significant temperature inversion associated with the anticyclonic subsidence and corresponds to an altitude of approximately 3 km, where haze layers were often observed.

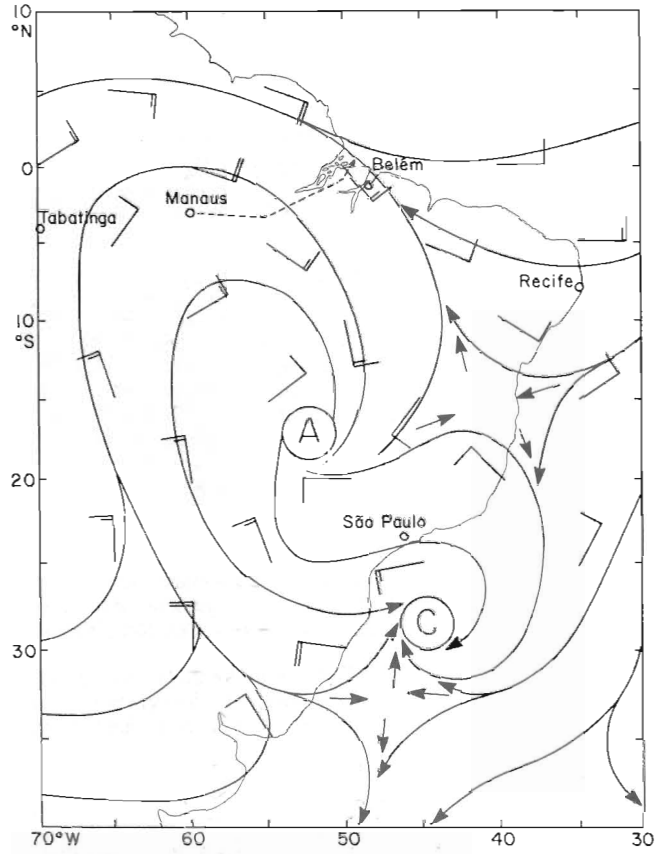

Fig. 1. Streamline map for the 700-mbar level over western South America on August 9, 1985 (1200 UT), showing wind directions and velocities and the position of the subtropical anticyclone (A) and a cyclone (C) off the east coast of Brazil. The track of flight 16 (August 8, 1985) is indicated as a dashed line.

Visual Observations of Atmospheric Haze

When the Electra aircraft entered the research area over central Amazonia on July 12, the visibility was excellent, and no haze layers were evident. Since a period of frequent, heavy rains had preceded our arrival, it is to be assumed that any previously existing haze would have been removed by washout and any layered structure destroyed by intense convective activity. No haze layers were seen on flights 3 and 4 (July 17 and 19). On flights 6 and 7 (July 23–24, survey flights to Belém and back) dense, brownish haze layers were seen between Manaus and about 50°–52°W at altitudes of about 1.5–2.5 km. These layers were typically only a few hundred meters thick and of considerable geographic extent (tens to hundreds of kilometers). During the following period, up to July 31 (flights 8 to 11), haze layers either were not observed or were related either to local burning in the Manaus area or to aerosol particle growth at high humidities. Flights 12 and 13 (August 2–3) were conducted under conditions of considerable cloudiness and precipitation as an organized weather system passed through the Manaus area. Dense haze layers were observed during these flights at about 2 km altitude, but they appeared to be related to regional burning in the Manaus area. On the survey flight to Tabatinga, at the western border of Brazil, pronounced haze layers were found throughout most of the region traversed, at altitudes of 2–3 km. The most intense haze (Plate 1) was seen during flight 16 (August 8), the second survey flight to Belém, where multiple layers were present between Manaus and the Xingu river (at about 52°W). These layers were again quite thin but covered large areas. On the return flight the

Plate 1. Haze layer, as seen from the cockpit of the NASA Electra aircraft on August 8, 1985, over the Xingu River at an altitude of about 3.7 km.

following day, these haze layers were poorly defined because of convective activity in the region.

In contrast to the high-altitude haze layers described previously, which were not related to any source visible from the aircraft, we observed numerous plumes from local biomass burning during almost all of the flights. These plumes were usually coming from small plots which were being burnt for agricultural purposes. They were seen most frequently near Manaus and Tabatinga and when approaching the coastal region near Belém.

Satellite Observations and Air Mass Trajectories

Setzer and Pereira [1986] analyzed 25 NOAA 8/9 advanced very high resolution radiometer (AVHRR) satellite images of the Amazon region taken between July 19 and August 9, 1985. Plumes from biomass fires along the southern and southeastern periphery of the rain forest region were evident on most images, with the frequency and areal extent of burning increasing markedly through the study period. In Figure 2, we present composites of the information derived from the satellite images: Figure 2*a* shows all the plumes observed during the period July 20–31; Figure 2*b* covers the period August 3–9. It must be emphasized that because of limitations in the satellite coverage and because of cloud cover, the data in Figure 2 represent a lower limit for the impact of biomass burning on the atmosphere over the Amazon Basin as visible from a satellite. On some of the images, as many as 1200 fires were visible and as much as 90,000 km^2 was covered by smoke.

Air mass trajectories were calculated using the data from the rawinsondes released in the Amazon region. These calculations show that the emissions from biomass burning are transported with the prevailing winds to the west and north, i.e., from the southern periphery of the basin into the Amazon Basin itself. The trajectory calculations suggest therefore that the haze layers observed during our flights over central Amazonia originate from biomass burning. This can best be demonstrated by the example of flight 16 on August 8, 1985. Analysis of the satellite image taken on August 7 shows widespread burning and resulting plumes in the north of the Mato Grosso region and in the south of the state of Pará. In Figure 3, we show the plumes observed on this satellite image, together with 24-hour isobaric (850 hPa) forward trajectories originating in the regions of biomass burning and the track of flight 16. These trajectories suggest that the plumes had traveled about 1000 km between their point of origin and the sampling area. The transport time is of the order of 1 day, implying average windspeeds of the order of 40–50 km h^{-1} at 850 hPa. Such a relatively short transport time is consistent with our observations that the haze layers tended to lose their identity during the afternoon as a result of convective overturn up to the trade wind inversion. Comparison between the observed altitudes of the haze layers and the vertical soundings shows that the layers are usually trapped near the trade wind inversion. The daily convective cycling up to and to a small extent through this inversion provides a mechanism for the injection into the boundary layer of materials derived from biomass burning.

Lidar Observations

The vertical structure and areal extent of the biomass-burning plumes were documented using airborne lidar. Haze layers showed up on the lidar soundings on most flights. Layers derived from biomass burning could be positively identified by a combination of remote sensing (using lidar) and in situ measurements. During the vertical penetration of the biomass-burning plumes, we consistently noted enhanced concentrations of CO, O_3, and other chemical parameters, as will be discussed in detail later. Once these layers were identified on the basis of their chemical signatures, they could be followed by lidar during the horizontal flight segments and their chemical characteristics probed again during the next spiral ascent or descent. The availability of up-looking and down-looking lidar data made it possible to follow the haze layers during horizontal flight segments, both in the boundary layer (up-looking lidar, aircraft altitude typically about 150 m) and in the free troposphere (down-looking lidar, aircraft usually at 4000 to 5000 m altitude).

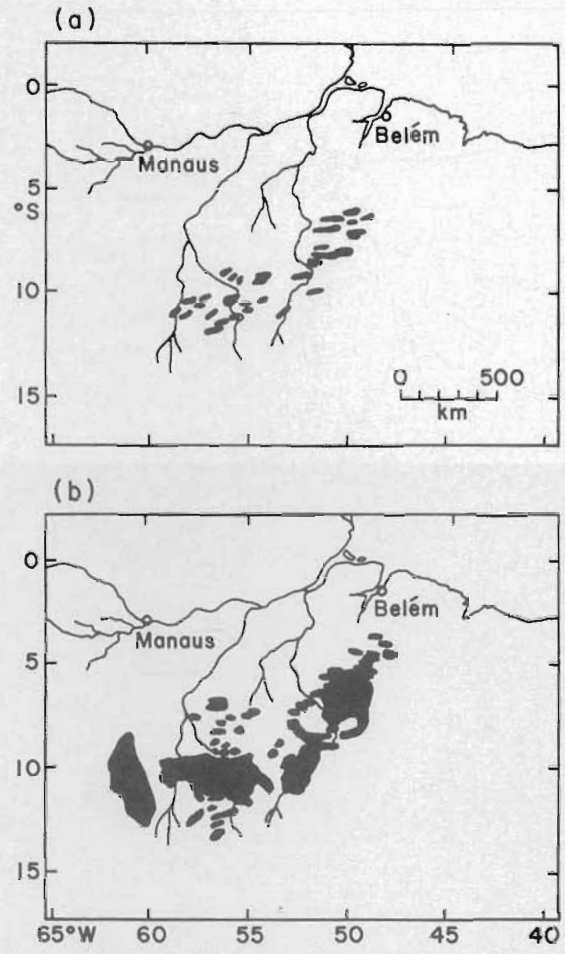

Fig. 2. Composite diagrams of burning plumes observed by satellite for the periods (*a*) July 20–31, 1985, and (*b*) August 3–9, 1985. All areas in which plumes were observed during these periods are plotted, regardless of the number of days the plumes were actually observed.

Plate 2 shows the lidar results obtained during flight 16 in the up-looking (Plate 2*a*) and down-looking (Plate 2*b*) mode for aerosols and in the down-looking mode using differential absorption lidar (DIAL) for ozone (Plate 2*c*). Plate 2*a*, which covers about 80 km of flight track, shows the areal extent and the vertical structure of the layers. Multiple layers were usually observed, stacked on top of one another and sepa-

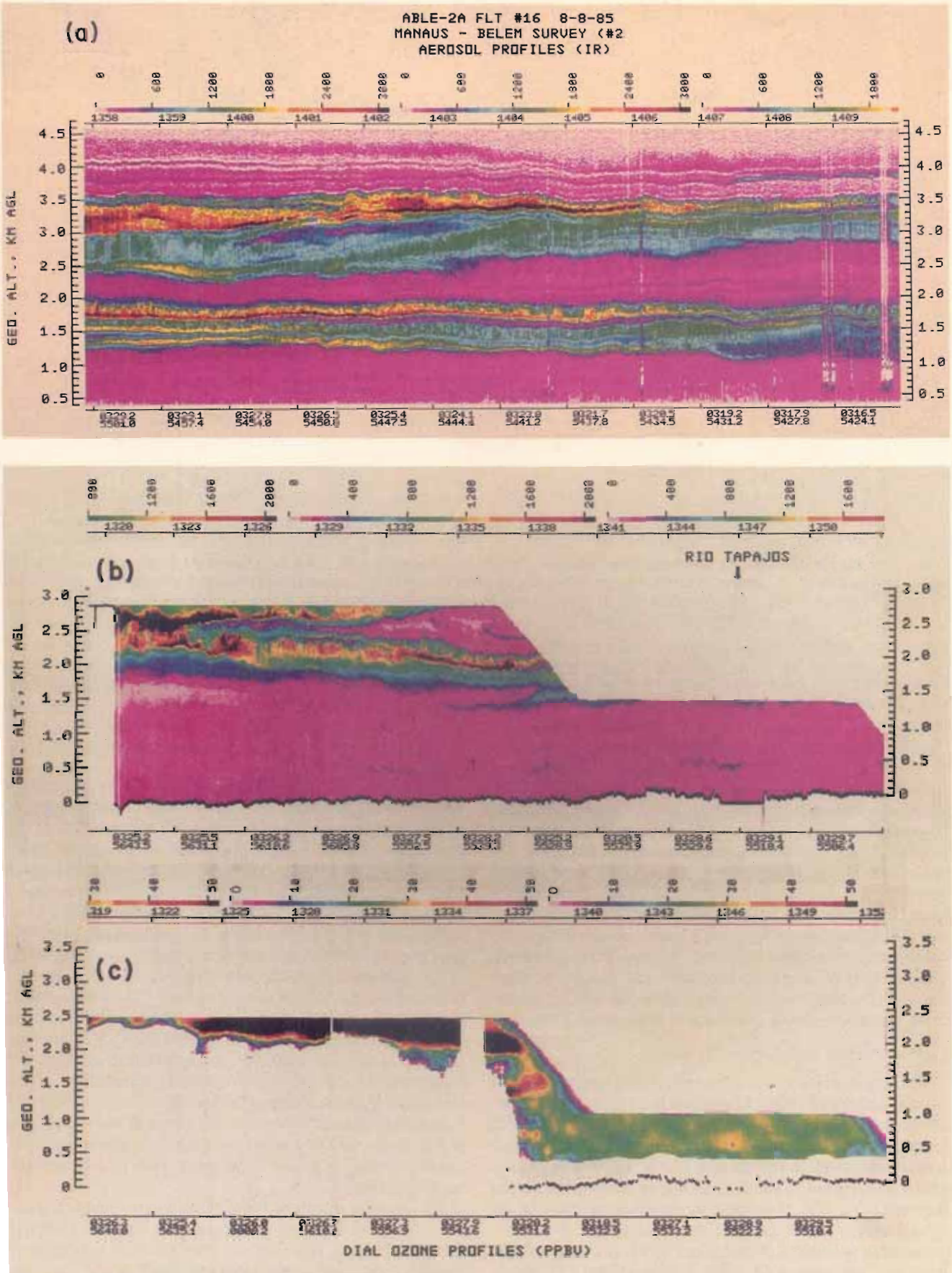

Plate 2. (*a*) Lidar profile taken in the up-looking mode from 1358 to 1410 UT on flight 16 from Manaus to Belém (August 8, 1985), showing the presence of multiple haze layers. (*b*) Down-looking lidar profile taken on the same flight, between 1320 and 1351 UT. (*c*) Ozone profile obtained by differential absorption lidar during the same time period as Plate 2*b*. (Note that because of optical limitations the upper altitude limit of the O_3 data is at a lower level than that of the light-scattering profile.)

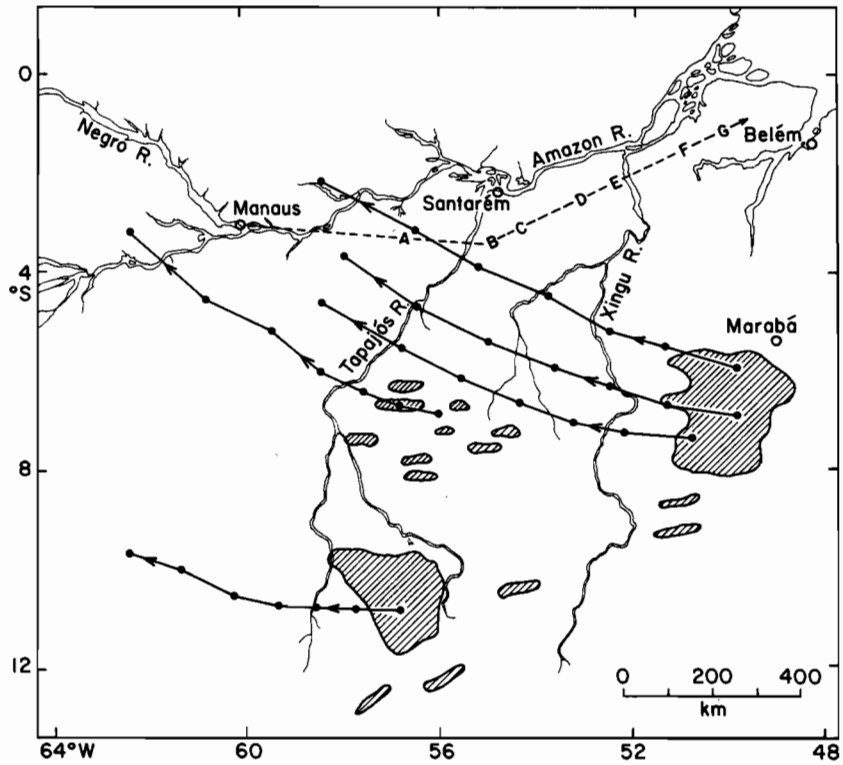

Fig. 3. Position of the burning plumes visible by satellite on August 7, 1985, and 24-hour isobaric forward air mass trajectories (850 hPa) from selected points in the burning areas. The dots on the trajectories indicate 4-hour time steps. The track of flight 16 on August 8, 1985, is indicated as a dashed line. The letters on the flight track indicate the positions of the vertical CO profiles shown in Figure 4.

rated by thin layers of clear air. Individual haze layers could often be followed for tens of kilometers. We assume that these layers represent the plumes from individual fires, which become stretched out by atmospheric transport processes at the level of their potential temperature.

Plates 2*b* and 2*c* show another segment from flight 16. The association between the light scattering by the haze particles (Plate 2*b*) and the presence of a pronounced O_3 maximum in the haze layer at about 2.3 km is clearly evident. The UV absorption by the haze layer is so strong that no reliable signal for the DIAL measurement of ozone could be obtained from below the layer. Examination of the lidar aerosol and ozone data shows that such ozone concentrations are consistently associated with the biomass-burning plumes. The ozone is the result of photochemical processes within the layers during their transport from the source region; these processes will be discussed in more detail later.

Carbon Dioxide and Carbon Monoxide

The major products of biomass combustion are carbon dioxide and water vapor. Consequently, CO_2 measurements can be used both to trace the burning plumes and to provide a master variable relating the concentrations of the diverse species observed in the plumes to the amount of organic matter combusted. This approach was limited by several factors. First, the absolute concentration of CO_2 in the atmosphere is relatively high; therefore a large increase is required to produce a plume signal which is clearly distinct from the background. Second, the levels of CO_2 in the boundary layer are naturally variable [*Wofsy et al.*, this issue], both temporally and spatially; as a result, it is difficult to detect CO_2 changes from dilute plumes. Finally, the CO_2 instrument flown on ABLE 2A proved to be sensitive to aircraft flight attitude, so that measurements during vertical soundings required careful control of aircraft maneuvers and frequent recalibration.

Carbon monoxide is a more reliable tracer of biomass burning. It is produced during incomplete combustion of organic matter and typically represents about 5–20% of the combusted organic carbon [*Crutzen et al.*, 1979, 1985; *Greenberg et al.*, 1984]. Consequently, the enhancement of CO in the plumes and haze layers relative to the atmospheric background is much easier to detect than that of CO_2, since the amount of CO in the emissions from biomass burning is only about 1 order of magnitude less than that of CO_2, while in the background air the concentration of CO is about 3 orders of magnitude lower than that of CO_2. Furthermore, the CO instrument showed no sensitivity to aircraft attitude and had a shorter response time than the CO_2 instrument [*Sachse et al.*, this issue]. We have therefore used the CO instrument as the primary source of information for the identification and tracking of the biomass-burning plumes. In Figure 4 we present the results of a series of vertical profiles of CO taken between Manaus and Belém during flight 16, which show the regional-scale distribution of the biomass-burning plumes.

We carefully examined those cases where reliable CO and CO_2 data were obtained simultaneously, in order to derive relative emission rates for the two species. In Figures 5 through 7 we present the simultaneous CO and CO_2 data from the haze layers sampled on flight 16. Figures 5 and 6 represent vertical soundings made at positions B and C

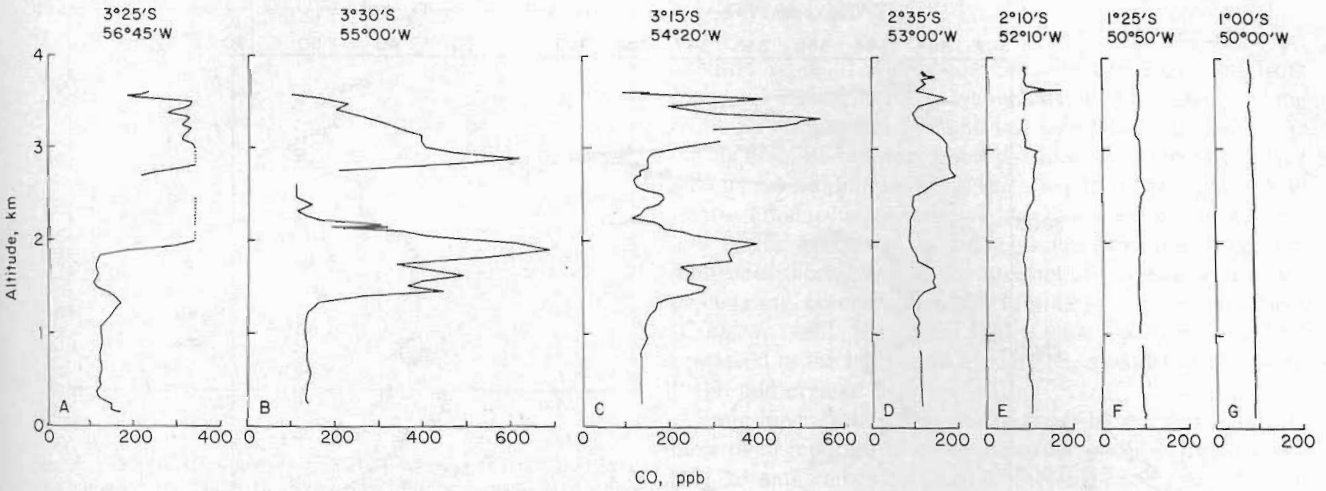

Fig. 4. Vertical profiles of CO concentration over the Amazon Basin between Manaus and Belém (flight 16, August 8, 1985). The sampling locations are indicated below the profiles: (*a*) 3° 25'S, 56° 45'W; (*b*) 3° 30'S, 55° 00'W; (*c*) 3° 15'S, 54° 20'W; (*d*) 2° 35'S, 53° 00'W; (*e*) 2° 10'S, 52° 10'W; (*f*) 1° 25'S, 50° 50'W; (*g*) 1° 00'S, 50° 00'W. The dotted lines in Figure 4*a* indicate that the instrument was outside of the calibrated range during this period.

(Figure 3), respectively. Within the haze layers near 2 and 3–3.5 km altitude, good correlation between the CO and CO_2 concentrations is evident. This correlation is, however, not apparent in the boundary layer (Figure 5), where CO_2 fluctuations are due mainly to exchange of CO_2 with the forest biota. Figure 7 shows data collected on a horizontal flight segment in which we attempted to collect aerosol and gas samples by flying continuously within a haze layer. The fluctuations in the trace gas concentrations evident in Figure 7 are due to the difficulty of maintaining the aircraft within these thin layers (cf. Plate 2). It is clear from these data that the results of integrated samples collected in the plumes over an extended period, as required for aerosol sampling, do not represent the concentrations in the center of the plume. However, if we integrate the CO data over the same period, we can use CO to normalize the data from integrated samples to either the concentrations in the center of the plume or to a "pure" smoke component.

In Figure 8 we have plotted 10-s averages of the CO_2 data from the haze layers sampled on flight 16 versus the corresponding CO values. A very good correlation is apparent. The correlations for the data sets from spiral 4B (representing the layer at about 2 km), from spiral 5 (representing the layer at about 3.3 km), and the horizontal sample at about 3.5 km are not significantly different from one another: the $\Delta CO/\Delta CO_2$ ratios (i.e., the slopes of the regression of CO on CO_2) are 0.088 ± 0.008, 0.080 ± 0.007, and 0.079 ± 0.006, respectively; the r^2 values in all cases are greater than 0.8. Pooling all data from flight 16, we obtain a $\Delta CO/\Delta CO_2$ ratio of 0.085 ± 0.004 with an r^2 of 0.82 (n = 112).

Examination of the CO data sets showed the presence of additional biomass-burning plumes during flights 3, 5, 6, 7, 9,

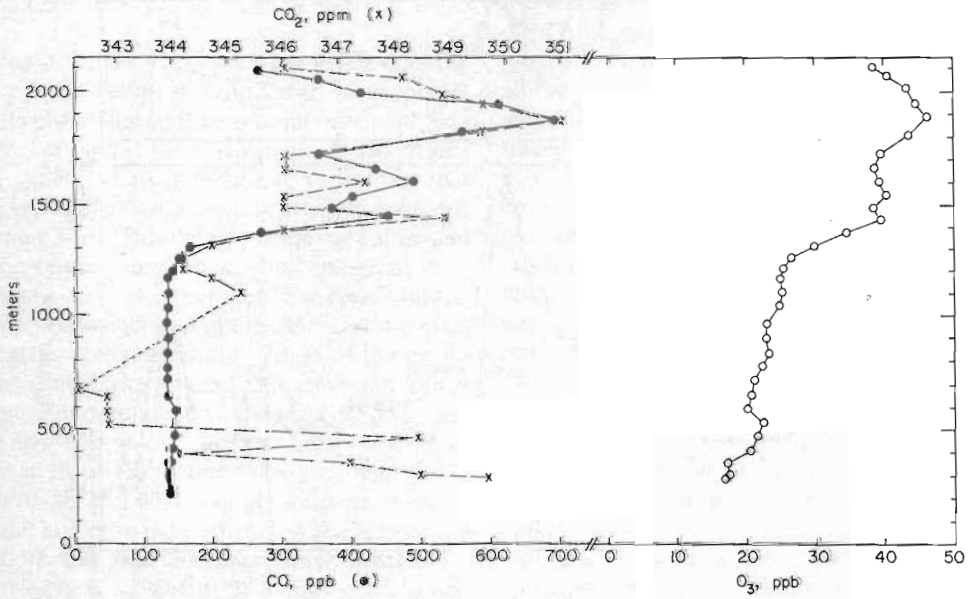

Fig. 5. Vertical profiles of CO, CO_2, and O_3 (10-s averages) at position B (Figure 3) on flight 16 (August 8, 1985).

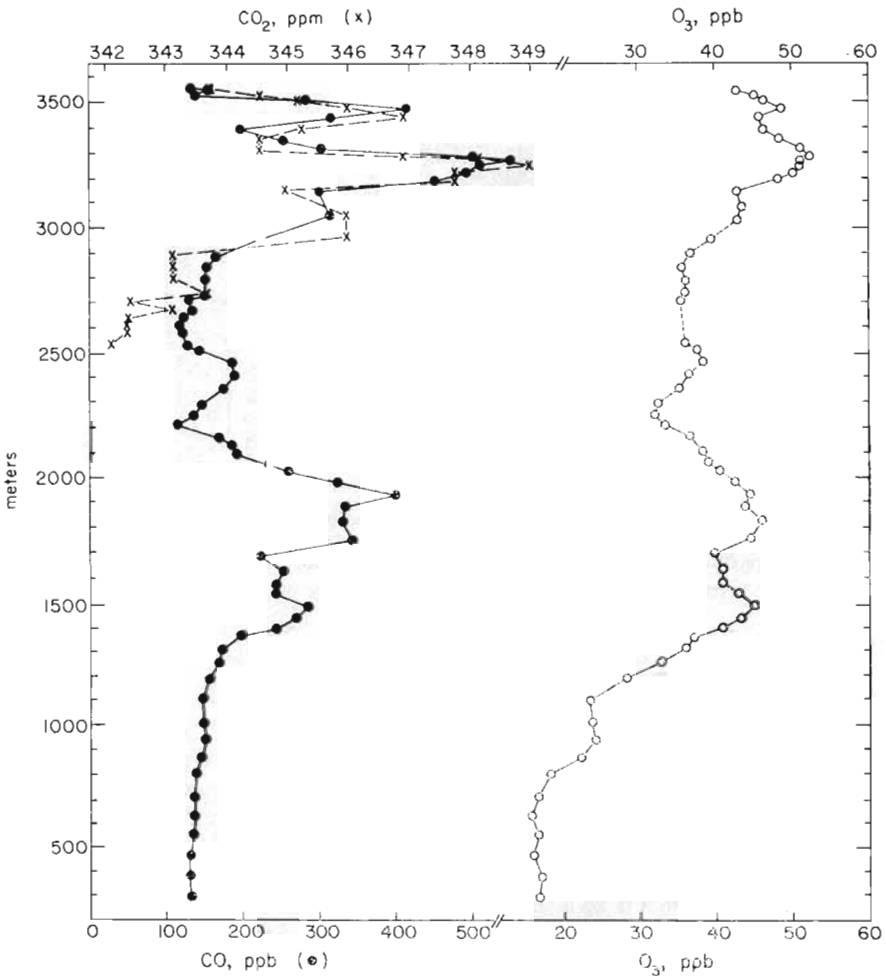

Fig. 6. Vertical profiles of CO, CO_2, and O_3 (10-s averages) at position C (Figure 3) on flight 16 (August 8, 1985).

10, 12, 13, 14, 16, and 17. However, many of these plumes resulted from local burning and were present within the boundary layer where the CO_2 concentrations are too variable to allow detection of the associated CO_2 enhancement. Therefore besides the data from flight 16 discussed earlier, simultaneous CO and CO_2 data from burning plumes were only available from flights 12, 14, and 17. On flight 12 there was a CO layer at about 2 km, just below the trade wind

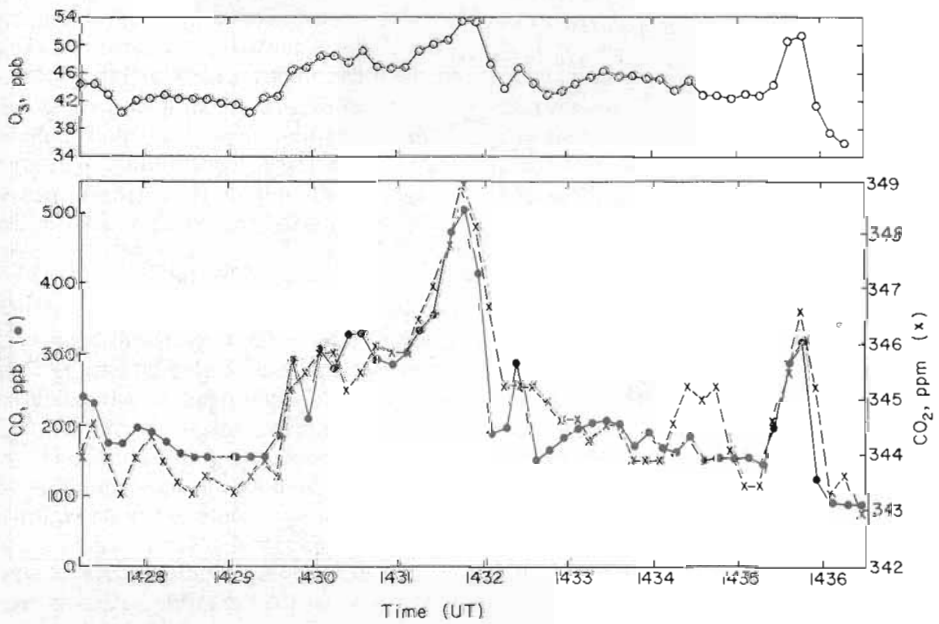

Fig. 7. CO, CO_2, and O_3 concentrations during level flight in a haze layer at 3.5-km altitude.

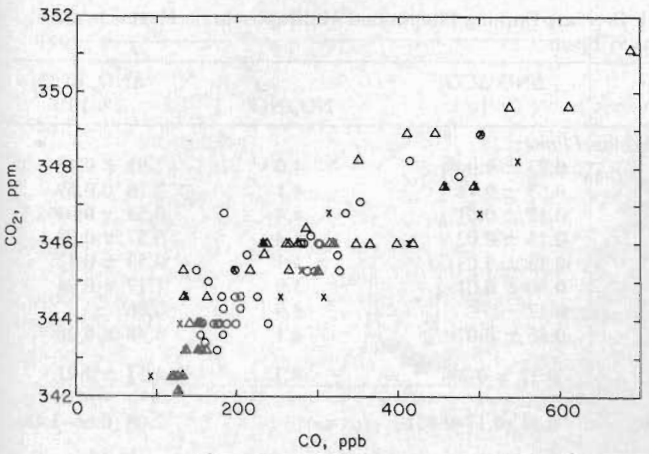

Fig. 8. Plot of CO_2 versus CO (10-s averages) from the haze layers sampled on flight 16. Triangles indicate spiral descent at position B (Figure 3); crosses indicate spiral climb at position C; circles indicate level flight at 3.5 km.

inversion. The CO_2 data show no clear increase in this layer, which, considering the resolution of our CO_2 instrument (0.6 ppm), places a lower limit of 0.15 on the $\Delta CO/\Delta CO_2$ ratio. On flight 14, from Manaus to Tabatinga, we sampled a series of haze layers between 2 and 3 km altitude which had a $\Delta CO/\Delta CO_2$ ratio of the order of 0.05. A similar ratio was observed in a haze layer at about 3 km altitude during flight 17, from Belém to Manaus. However, the precision to which the $\Delta CO/\Delta CO_2$ ratio could be estimated was very poor for these flights compared to the ratios from flight 16 because of the high variability of the background CO_2 concentrations relative to the signal from the plumes. These ratios are therefore not included in further calculations.

The $\Delta CO/\Delta CO_2$ emission ratios observed by us are within the range of literature data, which span values of 0.04–0.25 for grasslands and 0.03–0.21 for forest fires [*Darley et al.*, 1966, 1972; *Boubel et al.*, 1969; *Fritschen et al.*, 1970; *Gerstle and Kemnitz*, 1967; *Crutzen et al.*, 1979, 1985; *Greenberg et al.*, 1984]. In a series of experimental fireplace fires in which wood, brush, and leaves were burned, *Talbot et al.* [1988] measured $\Delta CO/\Delta CO_2$ ratios of 0.077 ± 0.046 ($n = 9$).

Our emission ratios tend to be somewhat lower than the mean obtained by the National Center for Atmospheric Research (NCAR) group during their measurements in Brazil in 1979 and 1980 (0.11–0.12 [*Crutzen et al.*, 1985; *Greenberg et al.*, 1984]). This may be due to the fact that much of the NCAR data is based on flask samples collected at individual burning sites. This type of sampling would tend to favor the lower-temperature, smoldering emissions over the high-temperature ones. In experimental fireplace burns, *Dasch* [1982] observed an increase in the CO/CO_2 ratio from about 0.09 during the high-temperature phase of the fire to over 0.25 in the smoldering stage. Our emission ratios measured in high-altitude plumes would tend to favor the emissions from the largest and hottest fires, which are carried to higher altitudes by plume buoyancy. Our mean $\Delta CO/\Delta CO_2$ ratio (0.085 ± 0.004) is in good agreement with the averages of the literature data other than those from the NCAR study: 0.07 and 0.06 for grass and forest fires, respectively [*Darley et al.*, 1966, 1972; *Boubel et al.*, 1969; *Fritschen et al.*, 1970; *Gerstle and Kemnitz*, 1967].

Nitric Oxide and NO_x

Nitric oxide is the major nitrogen oxide emitted from biomass burning. In the presence of sunlight, ozone, and the hydrocarbons which are emitted simultaneously with NO during biomass burning, photochemical reactions take place which lead within minutes to the presence of NO and NO_2 in photostationary state, followed by slower reactions equivalent to the processes in smog photochemistry. Since the midtropospheric haze layers were about 1 day old at the time of sampling, comparable to the lifetime of NO_x in the tropics [*Crutzen*, 1986], we expect that a large fraction of the NO produced in the burns had already been oxidized to HNO_3, PAN, and organic nitrates.

Emission ratios ($\Delta NO_x/\Delta CO_2$) from biomass combustion have been reported to be of the order of 10^{-3}: *Evans et al.* [1977] found values between 0.35×10^{-3} and 1.6×10^{-3} in fresh smoke from prescribed burning in Australia. The lowest values were measured in clearing burns in felled forest, the highest in grass and swamp flat fires. The emission ratio was clearly related to the N/C ratio in the fuel material. *Crutzen et al.* [1985] found a ratio of 2×10^{-3} in the boundary layer over Brazil. However, the data of Crutzen et al. are difficult to interpret, since they are taken outside of the plumes, so that some of the NO_x from burning may have been lost as a result of conversion to HNO_3, PAN, etc. On the other hand, their data would include contributions from soil emissions, which may be substantial in this region [*Keller et al.*, this issue]. An emission ratio of 2.8×10^{-3} has been measured from the burning of landscape refuse [*Gerstle and Kemnitz*, 1967], while wood burning in fireplaces and stoves tends to give emission ratios below 1×10^{-3}, presumably because of the lower nitrogen content of wood relative to leafy material [*Dasch*, 1982; *DeAngelis et al.*, 1980; *Cooper*, 1980; *Hao et al.*, 1987]. In contrast to the behavior of CO, the NO_x/CO_2 ratio does not change significantly during the combustion process and appears to be similar during the flaming and smoldering stages [*Dasch*, 1982]. It appears to depend almost exclusively on the nitrogen content of the fuel.

We calculated $\Delta NO/\Delta CO$ ratios by correlation analysis of the NO and CO data collected in biomass-burning plumes over Amazonia (Table 1). We separated our data into two groups, based on their relationship to visible sources and the altitude at which the plumes were present. We used the visual observation of local fires to which the plumes could be traced as evidence for "fresh" plumes, in which little conversion of emitted NO_x has yet taken place. The presence of haze layers at midtropospheric levels in the absence of local burning, on the other hand, suggests that they represent "aged" plumes, where a large part of the oxides of nitrogen have already been converted to HNO_3, PAN, and organic nitrates. On the basis of air mass trajectory calculations, the age of these haze layers appears to be of the order of 1–2 days.

The fresh burning plumes sampled during our flights could usually be seen to originate from local fires in plots of land that were being cleared for agricultural purposes (flights 3, 5, 14, 16, and 17). In the data these plumes show up as sharp spikes with a duration of only a few seconds (Figure 9). In two instances (flights 10 and 12) the samples were collected in the regional plume of the Manaus area and contain a mixture of fresh local plumes and more aged material.

TABLE 1. Ratios of ΔNO and ΔNO_x to ΔCO and ΔCO_2 in Fresh Biomass-Burning Plumes and Midtropospheric Haze Layers Over the Amazon Basin

Flight	Altitude, km	n	r^2	$\Delta NO/\Delta CO$ ($\times 10^3$)	$\Delta NO/\Delta CO_2$[a] ($\times 10^3$)	NO_x/NO[b]	$\Delta NO_x/\Delta CO_2$ ($\times 10^3$)
				Fresh Biomass-Burning Plumes			
3	0.25–0.5	97	0.74	8.59 ± 0.52	0.73 ± 0.04	4.0	2.92 ± 0.16
5	0.3	60	0.69	6.19 ± 1.69	0.53 ± 0.14	4.1	2.16 ± 0.59
10	0.15	319	0.53	1.41 ± 0.07	0.12 ± 0.01	4.4	0.53 ± 0.04
10	0.15	43	0.59	1.52 ± 0.20	0.13 ± 0.02	4.4	0.57 ± 0.08
12	1.6	14	0.52	1.50 ± 0.38	0.13 ± 0.03	4.1	0.53 ± 0.12
14	0.65	56	0.95	3.43 ± 0.10	0.30 ± 0.01	3.9	1.17 ± 0.04
16	0.13	...	...	2.0[c]	0.17[c]	3.9	0.66[c]
17	0.15	28	0.84	9.96 ± 0.85	0.85 ± 0.07	4.1	3.48 ± 0.28
Mean, all flights				4.32 ± 3.46	0.37 ± 0.29	4.1	1.51 ± 1.21
Mean (range) flights 3,5,14,16,17				6.0 (2.0–10.0)	0.51 (0.17–0.85)		2.08 (0.66–3.48)
				Aged Haze Layers			
7	2.2	65	0.79	1.03 ± 0.07	0.088 ± 0.006		
7	2.6–3.5	79	0.28	0.46 ± 0.08	0.039 ± 0.007		
14	2.7	59	0.51	0.44 ± 0.06	0.037 ± 0.005		
16	1.6–3.8	96	0.78	0.15 ± 0.01	0.013 ± 0.001		
Mean				0.52 ± 0.37	0.044 ± 0.031		

[a] Based on a $\Delta CO/\Delta CO_2$ ratio of 0.085.
[b] $NO_x = NO + NO_2$.
[c] No variance estimate possible, since the ratio was based on peak areas rather than the fast-response data, which were not available for this time period.

Consequently, we observed lower ΔNO and ΔCO values during these flights, and the CO and NO data were less closely correlated, as shown by lower values of r^2 (Table 1). We therefore consider the data from flights 3, 5, 14, 16, and 17 as most representative of the ΔNO/ΔCO ratio resulting from biomass burning in Amazonia (mean: 6.0×10^{-3}; range: $(2.0–10.0) \times 10^{-3}$).

To obtain an emission ratio for NO_x from these results, we multiplied the ΔNO/ΔCO ratio by the appropriate $\Delta CO/\Delta CO_2$ and NO_x/NO ratios. Using the $\Delta CO/\Delta CO_2$ ratio of 0.085 discussed earlier, we obtain a mean $\Delta NO/\Delta CO_2$ emission ratio of 0.51×10^{-3} (range: $(0.17–0.85) \times 10^{-3}$). The NO_x/NO ratios in each plume were obtained with a photochemical model calculation, using the chemical mechanism of *Lurmann et al.* [1986]. Starting from initial conditions representative of the burning area, the chemical evolution of the plume was followed over travel times ranging up to 30 min. The inputs of various hydrocarbons from the burning area were estimated from the measured value of ΔCO and the emission factors of *Greenberg et al.* [1984]. The composition of the background air was the same as that adopted by *Jacob and Wofsy* [this issue]. Ozone concentrations were taken from the aircraft data. Model calculations were conducted over single time steps, ranging from 1 to 30 min, using a backward Euler finite-difference scheme [*Richtmyer*, 1957] constrained to provide the observed amount of NO at the end of the time step. The NO_2 concentration was constrained to be at photochemical equilibrium with NO and PAN. We found that the NO_x/NO ratio was in the range 3.9–4.4 for all plumes and changed only slowly with time. In Table 1 we show the NO_x/NO ratio obtained from the model for each plume and the resulting $\Delta NO_x/\Delta CO_2$ ratios. The resulting mean $\Delta NO_x/\Delta CO_2$ ratio of 2.1×10^{-3} (using the values from the freshest plumes) is very close to the value of 2×10^{-3} reported by *Crutzen et al.* [1985].

As an example of the NO/CO relationship in the aged plumes represented by the midtropospheric haze layers, we show a scatter diagram for NO versus CO for all data from flight 16 (Figure 10). As observed for CO versus CO_2, the slope of the regression line, representing ΔNO/ΔCO, is the same for all the layers sampled. However, because of differences in the concentration of NO in the air surrounding the plumes, different intercepts are obtained for different layers. In Figure 10 the NO data have therefore been adjusted for the composition of the surrounding air by calculating the regression parameters for the data sets from each layer separately and then subtracting the NO intercept from the data. The mean ΔNO/ΔCO ratios obtained from all the aged haze layers probed during ABLE 2A are given in Table 1. The overall mean ΔNO/ΔCO ratio for these layers is 0.52 ± 0.37, 1 order of magnitude smaller than the ratio observed in the fresh plumes. This is strong evidence for the hypothesis that in the aged haze layers only a small fraction of the NO_x originally emitted in the burns is still present as NO_x and that the remainder has been converted to other nitrogen species or removed by aerosol formation or scavenging. Part of the converted NO_x is found as nitrate aerosol and HNO_3; in the aged haze layers their sum (the total nitrate concentration) is typically a few hundred parts per trillion (ppt) above the tropospheric background levels (Table 3), comparable to the concentration of NO_x in the fresh plumes. The remainder of the converted NO_x is probably present as organic nitrogen species, which were not determined in our study. This point will be discussed further in the section on emission flux estimates.

Ozone

Elevated ozone levels were consistently associated with the biomass-burning-derived haze layers in the free troposphere (Figures 5–7). Similar ozone maxima were observed by *Delany et al.* [1985] in vertical profiles taken over the

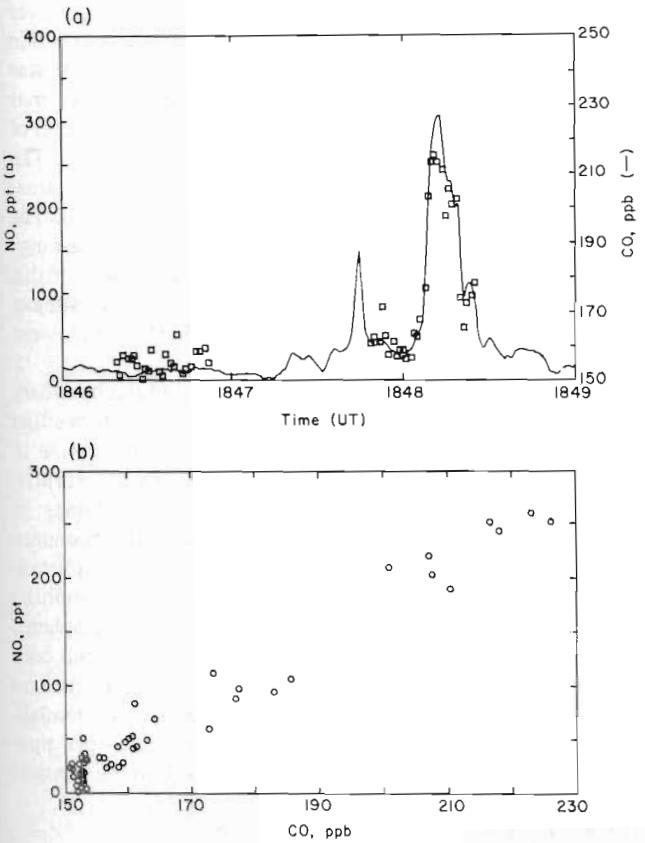

Fig. 9. (*a*) NO and CO concentrations (1-s averages) measured during the penetrations of a fresh biomass burning plume sampled on flight 14 (August 5, 1985) at about 0.65 km altitude. The NO data are intermittent because of the calibration cycles of the instrument. (*b*) Plot of NO versus CO from the same time period as Figure 9*a*.

cerrado region of Brazil. We interpret these elevated ozone levels as evidence for the photochemical formation of ozone in the plumes during transport from the source region. As discussed earlier, the transport time between the source and sampling area was of the order of 1 day, so that about 12 hours of sunlight were available for photochemical processes. We can therefore ignore photochemical ozone production by the oxidation of CH_4, which is too slow to make a significant contribution on this time scale, and assume that CO and nonmethane hydrocarbons (NMHC) are the main contributors to photochemical ozone production.

Oxidation of CO may either consume or produce O_3, depending on the amount of NO present. In the absence of NO, one molecule of O_3 is consumed per molecule of CO oxidized, whereas in the presence of relatively high amounts of NO, one molecule of O_3 is produced per molecule of CO oxidized. The crossover from O_3 consumption to O_3 production occurs at a NO/O_3 ratio of 0.2×10^{-3} [*Crutzen*, 1986]. Measured NO concentrations in the biomass-burning plumes ranged from 20 to 300 ppt, depending on the age of the plumes and the extent of dilution with surrounding air (see previous section). These values correspond to NO/O_3 ratios of $(0.4–6) \times 10^{-3}$, and we therefore assume that at least initially, the photochemical oxidation of CO took place in an ozone-producing regime. An upper limit for the amount of O_3 that may be produced from the excess CO in the plume is then given by

$$\Delta O_3 = k\,[OH]\,\Delta CO\,\Delta t$$

where k is the rate constant for the CO + OH reaction (2.2×10^{-13} cm^3 molecule^{-1} s^{-1}), [OH] is the concentration of OH (5×10^5 molecules cm^{-3} mean daytime value [*Jacob and Wofsy*, this issue]), and Δt is the time interval available for the reaction (12 hours). From this equation we obtain a value for $\Delta O_3/\Delta CO$ of about 0.005 on the basis of CO oxidation only. In contrast, the correlation analysis between the observed levels of O_3 and CO in the aged haze layers gave significantly larger $\Delta O_3/\Delta CO$ ratios, in the range of 0.01–0.09 (Table 2). This suggests that most of the O_3 production in the plumes is the result of the photochemical oxidation of NMHC.

In the fresh biomass-burning plumes, the O_3 enrichments were variable. The small smoke plumes on flights 16 and 17 had no detectable O_3 enrichment. The plume sampled in the Tabatinga area on flight 14 had a $\Delta O_3/\Delta CO$ ratio of 0.08 ± 0.02. The Manaus regional plume, which we probed on flight 10, had the highest O_3 enrichment, with a $\Delta O_3/\Delta CO$ ratio of 0.34 ± 0.03. This most likely reflects anthropogenic hydrocarbon emissions and the resulting smog chemistry in the Manaus region.

SO_2 and HNO_3

The concentrations of SO_2 and HNO_3 were determined by an impregnated filter technique [*Andreae et al.*, 1988]. The HNO_3 concentrations obtained on the K_2CO_3 impregnated filters must be considered upper limits, since it is possible that some reaction of organic nitrates, NO_x, etc., to HNO_3 may occur on the filters. However, together with the aerosol nitrate values discussed later, these values do give an indication of the amount of total nitrate (i.e., gas phase HNO_3 plus aerosol nitrate), since the potential artifacts are likely to be much smaller than the total nitrate values.

The results of the impregnated filter measurements are presented together with the aerosol data in Table 3. In contrast to the fast-response data reported earlier for CO, CO_2, NO, and O_3, these data represent integration for about 20–30 min, while the aircraft was trying to fly within the haze layer. This resulted in an effective dilution of the haze layer samples with ambient air, so that the concentrations given in Table 3 are not to be considered as the values representative of the center of the plumes. Consequently, the absolute

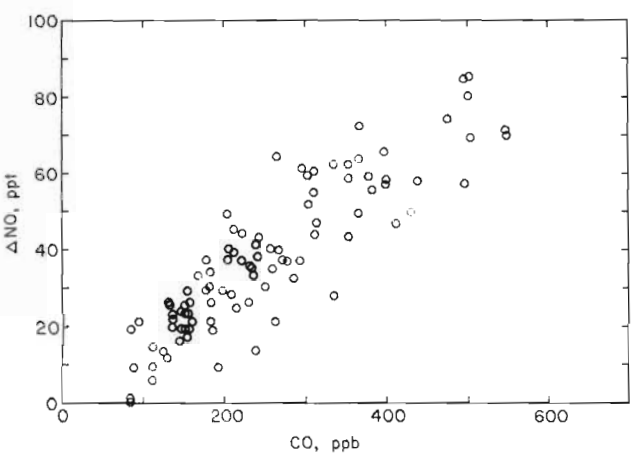

Fig. 10. Plot of the NO concentrations (adjusted for the concentrations in the air surrounding the haze layers; see text) versus CO from the haze layers sampled on flight 16.

TABLE 2. Correlation Between Ozone and Carbon Monoxide in Biomass-Burning Plumes Sampled on Flight 16 From Manaus to Belém on August 8, 1985

Altitude of Layer, km	Sampling Time, UT	$\Delta O_3/\Delta CO$, mol/mol	r^2	n
~1.5	1221–1245	0.060 ± 0.005	0.54	122
1.5–2.5	1340–1354	0.015 ± 0.010	0.68	74
1.5–2.5	1411–1415	0.060 ± 0.010	0.60	27
1.5–2.0	1445–1449	0.093 ± 0.010	0.89	13
~3.0	1338–1339	0.012 ± 0.001	0.98	5
3.0–3.5	1418–1422	0.027 ± 0.003	0.83	25
3.5–4.5	1316–1336	0.033 ± 0.004	0.50	62
3.5–4.5	1335–1336	0.019 ± 0.006	0.75	6
3.5–4.5	1419–1441	0.029 ± 0.002	0.70	132
3.5–4.5	1519–1520	0.087 ± 0.012	0.90	8

concentrations in Table 3 are not as informative as the ratios between the various chemical constituents. Later, we will attempt to reconstruct the chemistry of the plumes by scaling the integrated values to the integrated CO data obtained during the same sampling interval.

The samples in Table 3 were collected on three different flights and represent different types of plumes. The sample from the 1.7-km layer on flight 12 was taken near Manaus and probably represents the emissions from the Manaus region, where agricultural and domestic burning was widespread. In addition, some contributions from fossil fuel combustion may be present in this sample. The 1.3-km layer from flight 16 was imbedded within the cloud convection layer and was being mixed into the boundary layer. It was collected far from any potential source, and the air mas trajectories from this flight point to the southern perimeter of the Amazon Basin as the source region for this material. The 3.7-km layer from the same flight originates in the same area; it was, however, present above the convective region. The 3.0-km layer from flight 17 was also the result of long-range transport from the burning areas to the southeast, but this layer was again within the convective layer and was subject to active mixing. Many of the clouds in this area were precipitating.

Comparison between the haze layer data and the boundary layer and free troposphere averages in Table 3 shows that the haze layers are enriched in SO_2 and HNO_3 relative to both the boundary layer and the free troposphere. Surprisingly, SO_2 appears only weakly enriched in the plumes; in the sample from flight 12, it was actually below the boundary layer average. Since $SO_4^=$, on the other hand, is substantially enriched, we must assume that most of the SO_2 emitted in the burns has been oxidized to sulfate in the atmosphere. A dramatic enrichment of HNO_3 over the background conditions is found in all plumes except the 3.7-km layer on flight 16. Since in that layer the enrichment of particulate nitrate is most pronounced, it appears that a larger than usual fraction of total nitrate had partitioned into the aerosol.

TABLE 3. Concentations of SO_2, HNO_3 and Aerosol Components in the Biomass-Burning Plumes

	Flight 12	Flight 16	Flight 16	Flight 17	Boundary Layer	Free Troposphere
Altitude, km	1.7	1.3	3.7	3.0		
SO_2	5	79	43	39	27 ± 10	18 ± 16
$SO_4^=$ (aerosol)	416	265	223	304	129 ± 50	6 ± 7
MSA (aerosol)	9	12	18	17	5.9 ± 1.8	1.4 ± 0.7
ΣSO^a	430	360	280	360	160 ± 60	35 ± 24
HNO_3	250	220	82	570	65 ± 47	83 ± 83
NO_3^-	390	120	490	310	106 ± 53	18 ± 9
Total nitrate	640	340	570	880	170 ± 100	100 ± 90
NO	25	18	29	21	12–65	5–15
NO_x^b	88	63	102	74		
ΣNO^c	730	400	670	950		
NH_4^+	980	780	780	1070	290 ± 110	53 ± 22
Formate (aerosol)	39	43	90	103	24 ± 12	9.2 ± 5.5
Acetate (aerosol)	30	45	50	65	20 ± 12	7.8 ± 4.4
Oxalate (aerosol)	85	117	67	116	43 ± 16	5.0 ± 3.1
Pyruvate (aerosol)	5.5	6.7	11	13	3.8 ± 1.3	0.7 ± 0.7
Na	162	107	27	102	130 ± 65	26 ± 24
K	321	171	318	275	103 ± 38	20 ± 16
Cl	70	24	144	74	29 ± 24	20 ± 12
TPM,^{d} $\mu g\ m^{-3}$	10	12	6	ND	10 ± 8	2 ± 2
POC,^{e} $\mu g\ m^{-3}$	5.3	9.4	7.7	ND	8.8 ± 2.3	2.6 ± 0.7
EC,^{f} $\mu g\ m^{-3}$	1.6	1.1	1.0	ND	0.7 ± 0.3^g	ND
K/EC, mol/mol	0.10	0.078	0.16	ND		

Data are from integrated samples and do not represent peak concentrations. Mean values in the boundary layer and the free troposphere are given for comparison. All results are in parts per trillion by mole (ppt).

[a] $\Sigma SO = SO_2 + SO_4^= + MSA$.

[b] Estimated as 3.5 × NO.

[c] $\Sigma NO = HNO_3 + NO_3^- + NO_x$.

[d] TPM equals total particulate matter.

[e] POC equals particulate organic carbon.

[f] EC equals elemental (black) carbon.

[g] Filter samples collected at ground level within 100 km of Manaus.

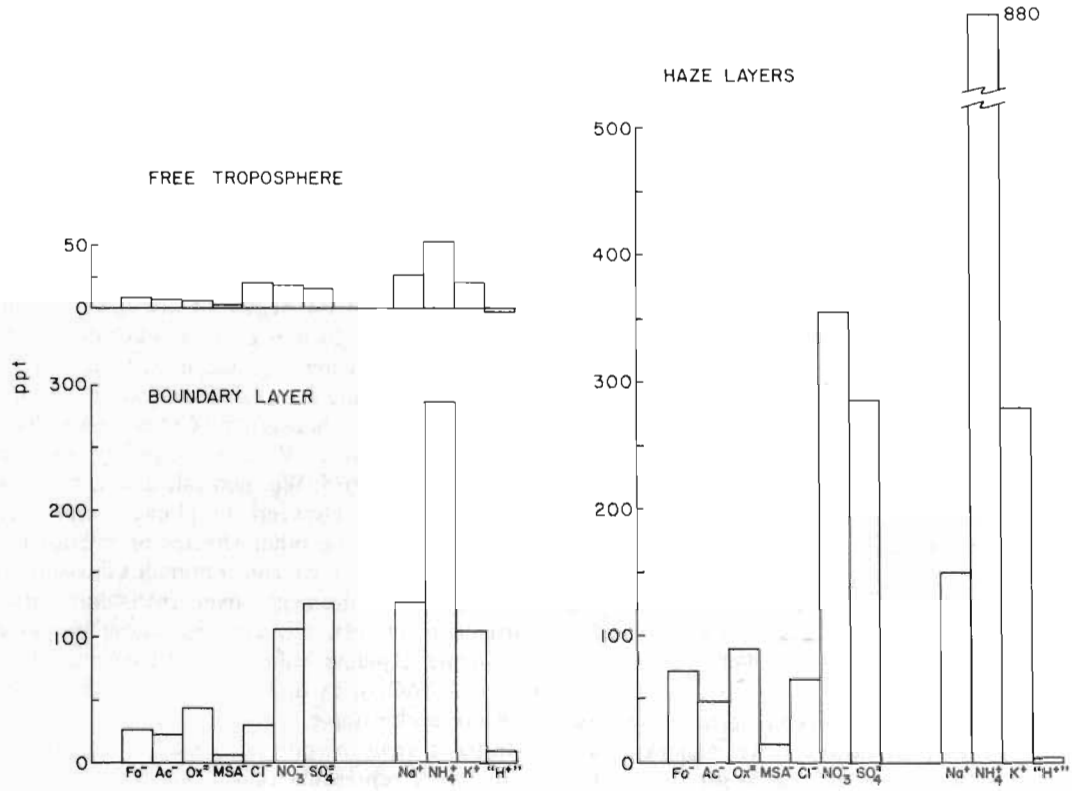

Fig. 11. Average aerosol ion concentrations in the boundary layer, the free troposphere, and the haze layers sampled during ABLE 2A. ("H^+" represents the difference between the cationic and anionic equivalent concentrations).

Aerosols

With the exception of sodium, all ionic aerosol constituents were found to be enriched in the biomass-burning plumes (Table 3). The degree of enrichment in the biomass-burning plumes versus the boundary layer aerosol is quite similar for all chemical species (except sodium): a factor of 2–3 on average. Surprisingly, particulate organic carbon (POC), which makes up most of the aerosol mass, shows no pronounced enrichment in the plumes. Soot (black) carbon is slightly enriched, but for this species the boundary layer data given in Table 3 are from ground sites within 100 km of Manaus (rather than from aircraft samples) and may reflect some influence of urban and agricultural emissions in the Manaus area. The ratio of potassium to black carbon in aerosols has been used as a tracer for biomass-burning-derived aerosols [*Andreae*, 1983; *Andreae et al.*, 1984]. In the haze layer samples this ratio was on average 0.11 (range 0.08–0.16), consistent with our previous measurements at the Ducke Reserve in 1982 (0.11), in the South American plume on Fernando de Noronha Island (0.11), and in the equatorial Atlantic (0.095) [*Andreae et al.*, 1984].

All organic acid ions are significantly enriched in the aerosols derived from biomass burning (Table 3). Formic and acetic acid are produced with emission ratios of $(6.9 \pm 4.2) \times 10^{-6}$ and $(69 \pm 36) \times 10^{-6}$, respectively, during the combustion of biomass [*Graedel et al.*, 1986; *Talbot et al.*, 1988]. They are probably also formed as atmospheric oxidation products of other organic compounds, e.g., formaldehyde and acetaldehyde, which are released during combustion with emission ratios of the order of $(0.1–0.5) \times 10^{-3}$ (mole aldehyde per mole C burned) [*Cooper*, 1980]. The presence of elevated levels of methanesulfonate in the biomass-burning aerosols was unexpected, since this species is usually considered to originate from the atmospheric oxidation of dimethylsulfide [*Andreae and Andreae*, this issue, and references therein]. Recent laboratory studies of biomass burning have shown, however, that this species is also released during biomass combustion (R. W. Talbot, unpublished data, 1986).

The chemical composition of the haze layer aerosol is quite similar to that of the boundary layer aerosol (Figure 11). This similarity poses a tantalizing problem: is biomass burning largely responsible for the production of the aerosol in the boundary layer over the Amazon Basin? The fact that POC (and total aerosol mass) is not enriched in the plumes indicates that there must be other sources, at least for this component, most likely emission by the forest vegetation. Furthermore, the ratio of total nitrate to total sulfur oxides (ΣSO, $SO_2 + SO_4^= + MSA$) is about twice as high in the plumes as in the boundary layer, so that the boundary layer aerosol could not be explained simply by dilution of burning-derived aerosol. Consequently, a sulfur source is required for the boundary layer in addition to biomass burning. In a companion paper [*Andreae and Andreae*, this issue], we have investigated the fluxes of biogenic sulfur gases to the boundary layer over the Amazon Basin and have concluded that they indeed represent an important, if not the dominant, source of this element. The absence of a sharp increase in the basinwide concentration of aerosol constituents [*Talbot et al.*, this issue] in spite of a dramatic increase in the incidence of burning at the southern perimeter of the Amazon Basin [*Setzer and Pereira*, 1986] argues against long-range transport of biomass-burning-derived aerosol as

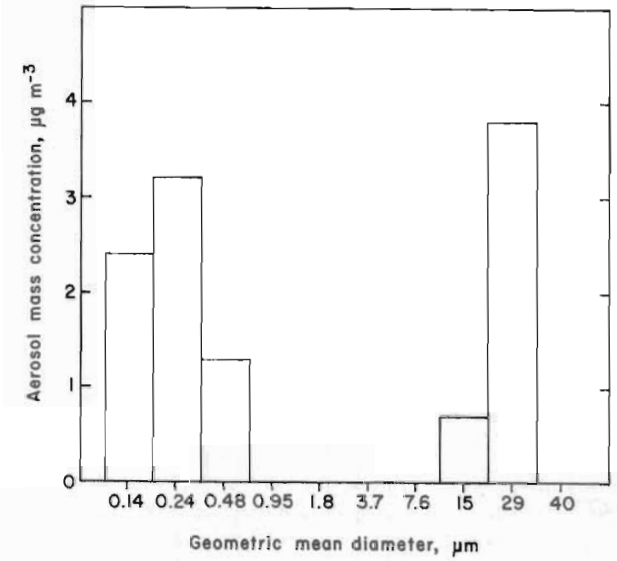

Fig. 12. Aerosol particle size distribution within the haze layer at 1.6 km altitude sampled on flight 16 (August 8, 1985), as determined by the quartz crystal microbalance impactor. The distribution shown is based on an average of 10 samples.

the major source of the boundary layer aerosol over the basin. On the basis of our data, however, we cannot exclude the possibility that local burns could still be responsible for much of the production of boundary layer aerosol. Conversely, boundary layer material becomes entrained in the biomass-burning plumes during the ascent of these plumes from the fires through the boundary layer into the midtroposphere. This effect would also lead to a convergence between the chemical compositions of the haze layer and boundary layer aerosols.

The total ionic charges of anions and cations in the plume aerosols balance each other within 5–10%. Organic acid anions contributed 9–25% of the anion sums, indicating that the aerosols were initially slightly alkaline, probably due to the presence of K_2CO_3. The main cationic species is NH_4^+ (followed by K^+). Since most of the emitted SO_2 and a large fraction of the NO_x appears to have been converted to the corresponding aerosol ions, sulfate and nitrate, and neutralized by ammonium ion, an emission of ammonia of about the same magnitude as that of NO_x and SO_2 from the fires is required to explain the observed aerosol composition.

The atmospheric aerosol in the haze layers contained both very large (20–30 μm) and fine (0.2–1 μm) particles at roughly equal mass concentrations (Figure 12). This size distribution was surprising in view of the large transport distances of these aerosols. Examination of the filters by scanning electron microscopy showed the presence of large, convoluted particles, which are presumably composed of organic matter and are likely to have a low density and, consequently, low settling velocities.

Emission Flux Estimates

We have estimated the emissions of carbon, nitrogen, and sulfur species and selected aerosol components from biomass burning on the basis of the concentration and enrichment ratios derived in the preceding sections. The ratio $\Delta CO/\Delta CO_2$ relates the amount of CO produced to the total amount of biomass combusted to CO_2. We have used the $\Delta CO/\Delta CO_2$ ratio of 0.085 calculated for flight 16 as the basis for estimating emission fluxes of other atmospheric species from biomass burning. While this value is based on data collected during one single flight, it does represent a total of 112 individual 10-s measurements collected throughout a large geographical range in the eastern Amazon Basin. These measurements therefore integrate over the emissions from a large burning area, with many individual fire sites and diverse burning conditions.

In Table 4 we summarize the calculations of emission ratios for various species based on the analysis of integrated samples collected on flights 14, 16, and 17, during time periods of about 20 min each in level flights in the haze layers. We calculated the mean ΔCO for each sampling period by averaging the CO concentration within the plume and subtracting the background CO concentration measured outside of the plume. We obtained ΔCO_2 from these values by dividing by 0.085. We then calculated the mean concentration difference between the plume sample and the surrounding air for the other species or species groups. For those species where we had continuous measurements (NO) or several measurements over the sample period (total particulate matter), we averaged these measurements to obtain mean plume values. We then calculated emission ratios ($\Delta X/\Delta CO_2$) by dividing by the ΔCO_2 value representative of each sample.

In the case of the nitrogen oxides, the ΔNO value in the haze layers represents only a small fraction of the total emitted NO_x, as discussed earlier. In order to test for agreement between the NO_x emission estimates derived from local plumes and the composition of the haze layers, we calculated the sum of NO_x and inorganic total nitrate ($\Sigma NO = NO_x + NO_3^- + HNO_3$) measured in the haze layers. If all of the NO_x emitted in the fires were present as these species, the emission ratio calculated as $\Delta\Sigma NO/\Delta CO_2$ from the haze layers should be the same as the $\Delta NO_x/\Delta CO_2$ ratio in the fresh plumes. Table 4 shows that in reality these ratios differ by a factor of 3: the mean $\Delta\Sigma NO/\Delta CO_2$ ratio from the haze layers is 0.63×10^{-3}; the $\Delta NO_x/\Delta CO_2$ ratio in the fresh plumes 2.1×10^{-3}. The difference in these values could be explained in part by the presence of PAN and organic nitrates, which would not have been detected in our measurements and which may be important odd nitrogen reservoir species within the haze layers. The presence of substantial amounts of PAN and organic nitrates in the atmospheric odd nitrogen pool has also been suggested previously by *Fahey et al.* [1986] based on their studies at Niwot Ridge, Colorado.

There are few data on the emission of ammonia from biomass burning [*National Academy of Sciences*, 1979]. Based on the data of *Miner* [1969], emission ratios ($\Delta NH_3/\Delta CO_2$) of 1.9×10^{-3} and 0.24×10^{-3} can be estimated for forest fires and wood combustion, respectively. In Table 4 we present lower limits for the ammonia emission from biomass burning based on the aerosol ammonium ion concentrations. Since we did not measure gaseous ammonia, we cannot include the fraction which was still present in the gas phase. We do, however, expect that significant amounts of gaseous ammonia were still present, since we always found the aerosol anions to be completely neutralized by ammonium ion. Table 4 shows that the lower limits calculated here are comparable to *Miner*'s [1969] results. These data suggest that the emission ratio for ammonia is between 1×10^{-3} and 2×10^{-3}, of the same order as the emission

TABLE 4. Emission Ratios From Biomass Burning Based on the Composition of Midtropospheric Haze Layers Over Amazonia

	Flight				
	12	16	16	17	Mean
Sample	12–4	16–2	16–4	17–3	
Date	AUG 2, 1985	AUG 8, 1985	AUG 8, 1985	AUG 9, 1985	
Altitude, km	1.7	1.3	3.7	3.0	
$\overline{CO}$, ppb	173	190	192	173	
CO (background), ppb	125	120	82	90	
ΔCO, ppb	48	70	110	83	
ΔCO_2 (= $\Delta CO/0.085$)	565	824	1294	976	
$\overline{NO}$, ppt	25	18	29	21	
NO (background), ppt	11	...	14	14	
ΔNO, ppt	14	...	15	7	
$\Delta NO/\Delta CO_2$, 10^{-3}	0.025[a]	0.014[b]	0.012[b]	0.007[a]	0.015
$\overline{\Sigma NO}$[c] ppt	700	390	640	930	
ΣNO (background), ppt	127	134	73	197	
$\Delta\Sigma NO$, ppt	573	256	567	733	
$\Delta\Sigma NO/\Delta CO_2$, 10^{-3}	1.01	0.31	0.44	0.75	0.63
$\overline{NH_4^+}$, ppt	980	780	780	1070	
NH_4^+ (background), ppt	242	108	22	132	
ΔNH_4^+, ppt	738	672	758	938	
$\Delta NH_4^+/\Delta CO_2$, 10^{-3}	1.31	0.82	0.59	0.96	0.92
$\overline{\Sigma SO}$[d], ppt	430	360	280	360	
ΣSO (background), ppt	122	103	22	154	
$\Delta\Sigma SO$, ppt	308	257	258	206	
$\Delta\Sigma SO/\Delta CO_2$, 10^{-3}	0.55	0.31	0.20	0.21	0.32
$\overline{K}$, ppt	321	171	318	275	
K (background)	85	84	19	68	
ΔK, ppt	236	87	299	207	
$\Delta K/\Delta CO_2$, 10^{-3}	0.42	0.11	0.23	0.21	0.24
$\overline{TPM}$[e,f], $\mu g\ m^{-3}$		12	6		
TPM (background), $\mu g\ m^{-3}$		...	≤2		
ΔTPM, $\mu g\ m^{-3}$		...	4–6		
$\Delta TPM/\Delta CO_2$, g [kg C]$^{-1}$	<35	18[g]	6–8	<20	12
$\overline{POC}$[f,h], $\mu g\ C\ m^{-3}$			7.7		
POC (background), $\mu g\ C\ m^{-3}$			2.6		
ΔPOC, $\mu g\ C\ m^{-3}$			5.1		
$\Delta POC/\Delta CO_2$	<19	<23	7.9	<20	7.9

[a] Based on regression of fast-response NO and CO data.
[b] Based on calculation of ΔNO from average plume concentration.
[c] $\Sigma NO = NO_x$ + aerosol NO_3^- + gaseous NHO_3.
[d] $\Sigma SO = SO_2$ + aerosol $SO_4^=$ + MSA.
[e] TPM equals total particulate matter.
[f] For TPM and POC, the plume enrichment could be calculated only for sample 16–4; the other values are upper limits (see text).
[g] Based on regression between TPM and CO data.
[h] POC equals particulate organic carbon.

ratio for nitrogen oxides (Table 1). Evidently, a considerable fraction of fuel nitrogen is volatilized as ammonia.

Delmas [1982] studied the nitrogen and sulfur emissions from the burning of savannas in tropical Africa by evaluation of the nitrogen and sulfur content of the biomass before and after burning. His results suggested that almost all of the nitrogen and carbon were volatilized. The N/C mole ratio in the savanna vegetation investigated by *Delmas* [1982] was 4.2×10^{-3}, and a similar ratio of total nitrogen to CO_2 would be expected to prevail in the emissions. Litter fall from trees in the tropics can have significantly higher nitrogen content, of the order of 12×10^{-3} [*Melillo and Gosz*, 1983], so that a N/C ratio of $(6–10) \times 10^{-3}$ would be reasonable for the fires which produced the plumes and haze layers over Amazonia. Our NO_x emission ratios would then be consistent with the NO_x burning yields of 10–20% observed by *Evans et al.* [1977]. The sum of our NO_x and NH_3 emission ratios ($\geq 3 \times 10^{-3}$) accounts for 30–50% of the nitrogen expected in the fuel. Further amounts of nitrogen could have been present in the plumes in the form of gaseous ammonia and organic nitrogen compounds.

The emission ratio for sulfur oxides was determined in an analogous fashion by summing SO_2 and aerosol sulfate (ΣSO). There are no previous field measurements of sulfur emissions from biomass burning (with the exception of COS). *Cooper* [1980] quotes an emission factor of 0.2 g SO_2 kg^{-1} wood from wood-burning stoves, which would correspond to a $\Delta SO_2/\Delta CO_2$ ratio of about 0.10×10^{-3}. This ratio is lower than our value of 0.32×10^{-3}, consistent with the lower sulfur content of wood compared with that of foliage

TABLE 5. Regional and Global Emissions From Biomass Burning

	$\Delta X/\Delta CO_2$ μmol/mol			South American Tropics, Tg element yr^{-1}	Global, Tg element yr^{-1}		
	Best	Min	Max	Best	Best	Min	Max
CO_2	...	...	...	527	3100	2000	4000
CO	85	60	160	45	264	120	640
POC[a]	7.9	...	20	4	24	...	80
EC	2.2	1.0	2.6	1.2	6.8	2.0	10
NO_x	2.1	0.66	3.5	1.3	7.6	1.5	16.3
NH_3[b]	0.92	0.59	1.3	0.6	3.3	1.4	6.1
ΣSO	0.32	0.20	0.55	0.5	2.6	1.1	5.9
K	0.24	0.11	0.42	0.4	2.4	0.7	5.5
TPM[c]	12	6	25	6.3	37	12	100
Ozone	4.8	1.0	7.9	10	59	8	126

[a] Estimate highly uncertain, since flux is based on only one measurement.
[b] This estimate is based only on the particulate NH_4^+ concentrations in the aerosol. The fluxes could be higher if substantial amounts of ammonia are present in the gas phase.
[c] Emission ratios are in units of g (kg C)$^{-1}$.

and branches. From *Delmas'* [1982] data on the burning yield for sulfur in savanna fires, an emission ratio of 0.16×10^{-3} can be calculated, also somewhat lower than our estimate.

Emission ratios for total particulate matter (TPM) and particulate organic carbon were difficult to obtain because these components were present in the boundary layer at concentrations often comparable to those in the plumes. Only for sample 16-4, which was completely surrounded by free tropospheric air, were we able to calculate excess TPM and POC with confidence. For another sample, 16-2, we could obtain an emission ratio based on the correlation between the TPM data from the quartz crystal microbalance impactor and the fast-response CO data. The emission ratios given in Table 4 are quite low compared with the emission factors suggested by *Seiler and Crutzen* [1980], who quote values of 10–25 g aerosol L^{-1} fuel for agricultural fires (corresponding to about 20–50 g (kg C)$^{-1}$), versus our value of about 12 g (kg C)$^{-1}$. Since this value is based on only two measurements, we have estimated upper limits for the TPM emission ratio for the other samples by assuming that the excess TPM concentration (ΔTPM) in the plumes would be 10 μg m^{-3}, an amount which would have certainly shown up as a significant difference from the background levels. From this calculation we obtain upper limits for the TPM emission ratio of about 20–35 g (kg C)$^{-1}$, which are also at the low end of the range estimated by Seiler and Crutzen. On the other hand, our values are in reasonable agreement with the emission estimates of *Stith et al.* [1981], who give values of 4, 8, and 40 g (kg C)$^{-1}$ for TPM emissions from forest fires in the Pacific Northwest. Further support for the validity of lower emission ratios than those suggested by Seiler and Crutzen comes from measurements of TPM emissions from wood stoves and fireplaces ($(2–53) \times 10^{-3}$ [*Cooper*, 1980]; $(11–38) \times 10^{-3}$ [*Dasch*, 1982]). However, since the emission rate of particulates is highly dependent on a number of variables, particularly the intensity of the fire, as expressed by the rate of combustion, and the presence of secondary combustion zones which can "burn out" particulates, it is difficult to assess if the values obtained under such conditions can be realistically compared with results from agricultural burning.

Since the POC concentrations were about the same as the total aerosol mass as determined by the quartz crystal microbalance impactor, our emission ratio for POC is essentially identical with that for TPM. We obtained an upper limit of about 20 g (kg C)$^{-1}$ for the POC emission ratio using an approach analogous to that described for TPM. This range is again consistent with the emission ratios for POC from fireplaces (9.3×10^{-3} [*Cooper*, 1980]; $(4–15) \times 10^{-3}$ [*Dasch*, 1982]).

We were not able to measure elemental carbon (EC) in the free troposphere and thus could not calculate ΔEC. Therefore we used the average EC/POC ratio of 0.13 in the haze layers and the estimates of the POC emission ratio to derive an emission ratio for EC of about 1×10^{-3} for sample 16-4, and an upper limit of 2.6×10^{-3} for other flights. Fireplace studies suggest a similar range of values: *Cooper* [1980] gives an emission ratio of 2.7×10^{-3}, *Dasch's* [1982] data suggest values in the range of $(1–10) \times 10^{-3}$. Our EC/POC ratio is surprisingly low: most laboratory burning studies give values of 20% or more [*Cooper*, 1980; *Dasch*, 1982]. This may be due to dilution of the burning-derived aerosols in the haze layers with biogenic organic aerosol entrained from the boundary layer during the plume formation.

Since potassium in fine aerosol particles has been proposed as an indicator of biomass burning in atmospheric aerosols, we calculated an emission ratio for this species. The mean value of $\Delta K/\Delta CO_2$ was 0.24×10^{-3}. From this value and the ratio of potassium to black carbon (0.11), we can calculate an estimate for the emission ratio for EC which is based on more data than the single sample 16-4 used earlier. The resulting estimate, 2.2×10^{-3} is a factor of 2 higher than that based on sample 16-4 and should be considered more reliable.

Estimates of Regional and Global Emissions From Biomass Burning

On the basis of the emission ratios calculated in previous sections, we have estimated the source fluxes from biomass burning in the South American tropics and worldwide (Table 5). We used *Seiler and Crutzen's* [1980] CO_2 emission flux from biomass burning (best estimate 3.1 Pg C yr^{-1}; range 2-4 Pg C yr^{-1}) and the fraction of biomass burning allocated to the South American tropics by the same authors (17%). We estimated a "best value" for the global flux based on the best estimate of the CO_2 emission and the emission ratios. The minimum and maximum fluxes are obtained by multiplying

the high and low estimate of the CO_2 flux with the high and low estimates of the emission ratios, and the ranges given in Table 5 are therefore probably quite conservative.

Our best estimate for the global emission of CO from biomass burning is 260 Tg C yr^{-1} or 0.62 Pg CO yr^{-1}. This is somewhat lower than *Greenberg et al.*'s [1984] estimate, who used a higher CO emission ratio, but well within the range estimated by *Crutzen et al.* [1979]: 0.24–1.66 Pg CO yr^{-1}, based on forest fires in Colorado. Our estimate of 0.62 Pg CO yr^{-1} is also consistent with the work of *Volz et al.* [1981], who calculated a total flux of CO from biomass burning and the oxidation of biogenic hydrocarbons of 1.1 Pg CO yr^{-1}, with about equal contributions from the two sources. Our flux estimate is in the lower part of the range estimated by *Seiler and Conrad* [1986]: 1.0 ± 0.06 Pg CO yr^{-1}.

Consistent with the low emission factors obtained for TPM, POC, and EC, our global emission estimates for these substances (37 Tg TPM yr^{-1}, 24 Tg POC yr^{-1}, 6.8 Tg EC yr^{-1}) are much lower than those proposed by *Seiler and Crutzen* [1980]. Even our upper limits tend to be below the lower limits of the ranges given by *Seiler and Crutzen* [1980]: 200–450 Tg yr^{-1} for TPM, of which about 90% is assumed to be carbon compounds, and 90–180 Tg yr^{-1} for elemental carbon. Again, we can only assume either that D. E. Ward's (personal communication, 1979), cited by *Seiler and Crutzen* [1980]) emission factors are not applicable to the burns we sampled in Brazil, or that most of the emitted particulate matter is not subject to long-range transport. Our POC emission estimate is also lower than that of *Duce* [1978], who proposed a value of 60 Tg yr^{-1} for the POC flux from forest fires and agricultural burning. On the other hand, *Cachier et al.* [1985] have estimated the POC flux in the submicron size fraction from the tropical regions, based on measurements in tropical Africa: about 12 Tg yr^{-1}. Since about 70% of biomass burning takes place in the tropics, and 50–80% of the aerosol mass was present as submicron size particles in their samples, this value is in reasonable agreement with our results.

Our estimate of the global NO_x source from biomass burning, 7.6 Tg N yr^{-1}, is very close to that of *Crutzen et al.* [1985], who suggested a value of 6 Tg N yr^{-1} to be emitted from tropical burning. Both estimates are closer to the lower end of the range of 4–24 Tg N(NO_x) yr^{-1} from biomass burning estimated by *Logan* [1983]. It is evident that biomass burning is a significant source of NO_x to the global atmosphere, of the same order as the production by lightning (11 Tg N yr^{-1} [*Galbally*, 1985]). For comparison, the global NO_x emission from fossil fuel combustion has been estimated to be near 20 Tg N yr^{-1} [*Logan*, 1983].

The global NH_3 budget remains difficult to estimate; *Galbally* [1985] suggested that global emissions are dominated by animal excreta and that the global average emission rate is about 0.4–1.0 g N m^{-2} yr^{-1} for agricultural land. This would correspond to a global source of about 6–16 Tg N yr^{-1}. Our data suggest that biomass burning can make a significant contribution (≥3.3 Tg N yr^{-1}) to the global ammonia cycle, especially if the plumes contained substantial amounts of gaseous ammonia, which we were not able to detect.

The rate of sulfur emission from biomass burning derived from our measurements over Amazonia corresponds to a global source flux of 2.6 Tg S yr^{-1}. This estimate is lower than previous ones, which were based on the total amount of biomass burnt, the sulfur content of this biomass, and an assumed burning yield. For example, *Andreae* [1985] has estimated a global flux of 7 Tg S yr^{-1} based on a global burning rate of 6.8 Pg dry matter yr^{-1}, a sulfur content of 0.2 weight percent, and a burning yield of 50%. The present value is the first one based on actual field measurements on emissions and should provide a much more realistic estimate. The global emissions of sulfur from the land and ocean biota have been recently estimated at ca 4.3 and 35 Tg S yr^{-1}, respectively [*Andreae*, 1986; *Andreae and Andreae*, this issue]. This suggests that biomass burning has to be considered as a major source of atmospheric sulfur in remote continental regions, especially in the tropics. On the basis of sulfur fluxes given by *Andreae and Andreae* [this issue], we estimate a biogenic source flux for the tropical American continent of about 1 Tg S yr^{-1}. While the biogenic flux is twice as large as the biomass-burning-derived flux for the same area (Table 5), the geographical and seasonal limitation of biomass burning suggests that it is the dominant sulfur source to the atmosphere in many tropical regions during the burning season. In our measurements of sulfur gas and aerosol species over Amazonia [*Andreae and Andreae*, this issue], we found an increase of SO_2 and aerosol sulfate concentrations coinciding with the onset of the burning season. We could not clearly show, however, that this increase was in fact related to the transport of burning-derived materials into central Amazonia.

In Table 5 we have also estimated the rate of ozone production from the photochemical processes in the plumes and haze layers. This represents only the ozone production during the first day or so, mostly due to the oxidation of the nonmethane hydrocarbons. The total ozone production from these reactions, about 60 Tg yr^{-1}, is about one tenth of the global average of the stratospheric inputs or the rate of surface destruction [*Crutzen*, 1986]. In view of the regional distribution of biomass burning, which occurs predominantly in the tropics, we concur with the view of *Delany et al.* [1985] and *Crutzen et al.* [1985], who suggest that ozone production due to biomass burning is a significant contributor to the atmospheric ozone cycle, particularly in the tropics. The impact of O_3 from biomass burning on the regional atmosphere is quite evident from the observed O_3 profiles (Figures 5–7), which show that the ozone content in the aged plumes was 2–3 times higher than in the background atmosphere.

CONCLUSIONS

During a series of flights over the Amazon Basin with a highly instrumented aircraft, we have obtained data on the chemical composition of fresh and aged biomass-burning plumes derived from agricultural activities in Amazonia and at the southern perimeter of the basin. Biomass burning produced widespread haze over the Amazon Basin, which at times seriously reduced visibility. Large burning plumes originated at the southern perimeter of the basin and spread initially as multiple, thin layers at 2–5 km altitude. During the day, convective activity mixed material from these haze layers down into the boundary layer and to a limited extent up into the free troposphere.

The simultaneous operation of multiple fast-response chemical sensors, coupled with the collection of integrated samples for species for which no fast sensors were available,

proved to be a highly effective approach for the characterization of the plumes. As a result, we were able to derive emission ratios for carbon, nitrogen, and sulfur species, and several aerosol constituents, relative to CO_2. On the basis of these data, we have shown that substantial amounts of CO, particulate organic carbon, elemental carbon, NO_x, NH_3, and sulfur oxides are emitted during biomass burning. Our estimates of particulate matter, particulate organic carbon, and elemental carbon are substantially lower than some previous estimates, while our source fluxes for NO_x are in good agreement with the work of other authors. We present the first estimates for the biomass-burning flux of NH_3 and sulfur oxides based on field measurements and show these fluxes to be important in the global cycles of NH_3 and sulfur. Ozone production as a result of biomass burning contributes significantly to the regional ozone budget during the burning season.

Acknowledgments. We acknowledge the permission of the Government of Brazil to conduct this research in Brazil. We gratefully acknowledge the scientific and logistical collaboration of the Instituto de Pesquisas Espaciais (INPE), with special thanks to L. Molion. The cooperation of the flight crew of the NASA Electra research aircraft is gratefully acknowledged. T. Andreae helped with the analysis of the aerosol and impregnated filter samples and H. Buchan with the NO measurements. The assistance of S. Greco and J. Scala is greatly appreciated. We thank C. Butler, L. Overbay, W. McCabe and N. McRae for their assistance in the airborne lidar measurements of aerosol and ozone distributions. We also thank M. Dancy for help with the preparation of the manuscript and figures. This research was supported by the NASA Tropospheric Chemistry Program and NSF grant ATM-8407137.

REFERENCES

Andreae, M. O., Soot carbon and excess fine potassium: Long-range transport of combustion-derived aerosols, *Science, 220*, 1148–1151, 1983.

Andreae, M. O., The emission of sulfur to the remote atmosphere, in *The Biogeochemical Cycling of Sulfur and Nitrogen in the Remote Atmosphere*, edited by J. N. Galloway, R. J. Charlson, M. O. Andreae and H. Rodhe, pp. 5–25, D. Reidel, Hingham, Mass., 1985.

Andreae, M. O., The ocean as a source of atmospheric sulfur compounds, in *The Role of Air-Sea Exchange in Geochemical Cycling*, edited by P. Buat-Ménard, pp. 331–362, D. Reidel, Hingham, Mass., 1986.

Andreae, M. O., and T. W. Andreae, The cycle of biogenic sulfur compounds over the Amazon Basin, 1, Dry season, *J. Geophys. Res.*, this issue.

Andreae, M. O., T. W. Andreae, R. J. Ferek, and H. Raemdonck, Long-range transport of soot carbon in the marine atmosphere, *Sci. Total Environ., 36*, 73–80, 1984.

Andreae, M. O., H. Berresheim, T. W. Andreae, M. A. Kritz, T. S. Bates, and J. T. Merrill, Vertical distribution of dimethylsulfide, sulfur dioxide, aerosol ions, and radon over the northeast Pacific Ocean, *J. Atmos. Chem., 6*, 149–173, 1988.

Andreae, M. O., R. W. Talbot, T. W. Andreae, and R. C. Harriss, Formic and acetic acid over the central Amazon region, Brazil, 1, Dry season, *J. Geophys. Res.*, this issue.

Boubel, R. W., E. F. Darley, and E. A. Schuck, Emissions from burning grass stubble and straw, *J. Air Pollut. Control Assoc., 19*, 497–500, 1969.

Browell, E. V., G. L. Gregory, R. C. Harriss, and V. W. J. H. Kirchhoff, Tropospheric ozone and aerosol distributions across the Amazon Basin, *J. Geophys. Res.*, this issue.

Cachier, H., P. Buat-Ménard, M. Fontugne, and J. Rancher, Source terms and source strengths of the carbonaceous aerosol in the tropics, *J. Atmos. Chem., 3*, 469–489, 1985.

Cooper, J. A., Environmental impact of residential wood combustion emissions and its implications, *J Air. Pollut. Control Assoc., 30*, 855–861, 1980.

Crutzen, P. J., The role of the tropics in atmospheric chemistry, in *The Geophysiology of Amazonia*, edited by R. E. Dickinson, pp. 107–130, John Wiley, New York, 1986.

Crutzen, P. J., L. E. Heidt, J. P. Krasnec, W. H. Pollock, and W. Seiler, Biomass burning as a source of the atmospheric gases CO, H_2, N_2O, NO, CH_3Cl and COS, *Nature, 282*, 253–256, 1979.

Crutzen, P. J., A. C. Delany, J. Greenberg, P. Haagenson, L. Heidt, R. Lueb, W. Pollock, W. Seiler, A. Wartburg, and P. Zimmerman, Tropospheric chemical composition measurements in Brazil during the dry season, *J. Atmos. Chem., 2*, 233–256, 1985.

Darley, E. F., F. R. Burleson, E. H. Mateer, J. T. Middleton, and V. P. Osterli, Contribution of burning of agricultural wastes to photochemical air pollution, *J. Air Pollut. Control Assoc. 11*, 685–690, 1966.

Darley, E. F., H. E. Biswell, G. Miller, and J. Gross, Air pollution from forest and agricultural burning, paper presented at Spring meeting of Western States Section, Combust. Inst., Seattle, Wash., April 1972.

Dasch, J. M., Particulate and gaseous emissions from wood-burning fireplaces, *Environ. Sci. Technol., 16*, 639–645, 1982.

DeAngelis, D. G., D. S. Ruffin, J. A. Peters, and R. B. Reznik, Source Assessment: Residential Combustion of Wood, *EPA-600/2-80-042b*, Environ. Prot. Agency, Washington, D.C., 1980.

Delany, A. C., P. Haagenson, S. Walters, and A. F. Wartburg, Photochemically produced ozone in the emission from large-scale tropical vegetation fires, *J. Geophys. Res., 90*, 2425–2429, 1985.

Delmas, R., On the emission of carbon, nitrogen and sulfur in the atmosphere during bush fires in intertropical savannah zones, *Geophys. Res. Lett., 9*, 761–764, 1982.

Duce, R. A., Speculations on the budget of particulate and vapor phase nonmethane organic carbon in the global troposphere, *Pure Appl. Geophys., 116*, 244–273, 1978.

Evans, L. F., I. A. Weeks, A. J. Eccleston, and D. R. Packham, Photochemical ozone in smoke from prescribed burning of forests, *Environ. Sci. Technol., 11*, 896–900, 1977.

Fahey, D. W., G. Hübler, D. D. Parrish, E. J. Williams, R. B. Norton, B. A. Ridley, H. B. Singh, S. C. Liu, and F. C. Fehsenfeld, Reactive nitrogen species in the troposphere: Measurements of NO, NO_2, HNO_3, particulate nitrate, peroxyacetyl nitrate (PAN), O_3, and total reactive odd nitrogen (NO_y) at Niwot Ridge, Colorado, *J. Geophys. Res., 91*, 9781–9793, 1986.

Fritschen, L., H. Bovee, and K. Buettner, Slash fire atmospheric pollution, *Pap. PNW-97*, USDA Forest Serv., Pac. Northwest Forest and Range Exp. Sta., Portland, Oreg., 1970.

Galbally, I. E., The emission of nitrogen to the remote atmosphere, in *The Biogeochemical Cycling of Sulfur and Nitrogen in the Remote Atmosphere*, edited by J. N. Galloway, R. J. Charlson, M. O. Andreae, and H. Rodhe, pp. 27–53, D. Reidel, Hingham, Mass., 1985.

Garstang, M., et al., Trace gas exchanges and convective transports over the Amazonian rain forest, *J. Geophys. Res.*, this issue.

Gerstle, R. W., and D. A. Kemnitz, Atmospheric emissions from open burning, *J. Air Pollut. Control Assoc. 17*, 324–327, 1967.

Graedel, T. E., D. T. Hawkins, and L. D. Claxton, *Atmospheric Chemical Compounds: Sources, Occurrence and Bioassay*, Academic, Orlando, Fla., 1986.

Greenberg, J. P., P. R. Zimmerman, L. Heidt, and W. Pollock, Hydrocarbon and carbon monoxide emissions from biomass burning in Brazil, *J. Geophys. Res., 89*, 1350–1354, 1984.

Gregory, G. L., E. V. Browell, and L. S. Warren, Boundary layer ozone: An airborne survey above the Amazon Basin, *J. Geophys. Res.*, this issue.

Hao, W. M., S. C. Wofsy, M. B. McElroy, J. M. Beer, and M. A. Toqan, Sources of atmospheric nitrous oxide from combustion, *J. Geophys. Res., 92*, 3098–3104, 1987.

Harriss, R. C., et al, The Amazon Boundary Layer Experiment (ABLE 2A): Dry season 1985, *J. Geophys. Res.*, this issue.

Jacob, D. J., and S. C. Wofsy, Photochemistry of biogenic emissions over the Amazon forest, *J. Geophys. Res.*, this issue.

Keller, M., W. A. Kaplan, S. C. Wofsy, and J. M. da Costa, Emissions of N_2O from tropical forest soils: Response to fertilization with NH_4^+, NO_3^-, and PO_4^{3-}, *J. Geophys. Res.*, this issue.

Logan, J. A., Nitrogen oxides in the troposphere: Global and regional budgets, *J. Geophys. Res., 88*, 10,785–10,807, 1983.

Lurmann, F. W., A. C. Lloyd, and R. Atkinson, A chemical

mechanism for use in long-range transport/acid deposition computer modeling, *J. Geophys. Res.*, *91*, 10,905–10,936, 1986.

Martin, C., D. Fitzjarrald, M. Garstang, A. P. Oliveira, S. Greco, and E. Browell, Structure and growth of the mixing layer over the Amazonian rain forest, *J. Geophys. Res.*, this issue.

Melillo, J. M., and J. R. Gosz, Interactions of biogeochemical cycles in forest ecosystems, in *The Major Biogeochemical Cycles and Their Interactions*, edited by B. Bolin and R. B. Cook, pp. 177–222, John Wiley, New York, 1983.

Miner, S., Preliminary air pollution survey of ammonia, *Rep. APTD-69-25*, 39 pp., Nat. Air Pollut. Control Admin. Raleigh, N.C., 1969.

National Academy of Sciences, *Ammonia*, 384 pp., University Park Press, Baltimore, Md., 1979.

Richtmyer, R. D., *Difference Methods for Initial-Value Problems*, 238 pp., Wiley-Interscience, New York, 1957.

Sachse, G. W., R. C. Harriss, J. Fishman, G. F. Hill, and D. R. Cahoon, Carbon monoxide over the Amazon region during the 1985 dry season, *J. Geophsy. Res.*, this issue.

Seiler, W., and R. Conrad, Contribution of tropical ecosystems to the global budgets of trace gases, especially CH_4, H_2, CO and N_2O, in *The Geophysiology of Amazonia*, edited by R. E. Dickinson, pp. 133–160, John Wiley, New York, 1986.

Seiler, W., and P. J. Crutzen, Estimates of gross and net fluxes of carbon between the biosphere and the atmosphere from biomass burning, *Clim. Change*, *2*, 207–247, 1980.

Setzer, A. W., and M. C. Pereira, Detection of large biomass burning in the Amazon with satellite images, *Eos Trans. AGU*, *67*, 247, 1986.

Stith, J. L., L. F. Radke, and P. V. Hobbs, Particle emissions and the production of ozone and nitrogen oxides from the burning of forest slash, *Atmos. Environ.*, *15*, 73–82, 1981.

Talbot, R. W., M. O. Andreae, T. W. Andreae, and R. C. Harriss, Regional aerosol chemistry of the Amazon Basin during the dry season, *J. Geophys. Res.*, this issue.

Talbot, R. W., K. M. Stein, R. C. Harriss, and W. R. Cofer, Atmospheric geochemistry of formic and acetic acids at a mid-latitude temperate site, *J. Geophys. Res.*, *93*, 1638–1652, 1988.

Torres, A. L., and H. Buchan, Tropospheric nitric oxide measurements over the Amazon Basin, *J. Geophys. Res.*, this issue.

Volz, A., D. H. Ehhalt, and R. G. Derwent, Seasonal and latitudinal variation of ^{14}CO and the tropospheric concentration of OH radicals, *J. Geophys. Res.*, *86*, 5163–5171, 1981.

Wofsy, S. C., R. C. Harriss, and W. A. Kaplan, Carbon dioxide in the atmosphere over the Amazon Basin, *J. Geophys. Res.*, this issue.

M. O. Andreae, Max Planck Institute for Chemistry, Postfach 3060, D-6500 Mainz, Federal Republic of Germany.

E. V. Browell, G. L. Gregory, R. C. Harriss, G. F. Hill, G. W. Sachse, and R. W. Talbot, NASA Langley Research Center, Hampton, VA 23665.

M. Garstang, Department of Environmental Sciences, University of Virginia, Charlottesville, VA 22903.

D. J. Jacob and S. C. Wofsy, Center for Earth and Planetary Physics, Harvard University, Cambridge, MA 02138.

M. C. Pereira, Department of Meteorology, Instituto de Pesquisas Espaciais, C.P. 515, 12201 São José dos Campos, São Paulo, Brazil.

P. L. Silva Dias, Department of Meteorology, University of São Paulo, C.P. 30627, 01051 São Paulo, São Paulo, Brazil.

A. L. Torres, NASA Wallops Flight Facility, Wallops Island, VA 23337.

(Received January 8, 1987;
revised May 5, 1987;
accepted May 6, 1987.)